Doctral Thesis
博士論文

Study on Ionosphere Delay Correction for Multi-GNSS Positioning
マルチ GNSS 測位のための電離圏遅延補正に関する研究

March 24, 2017
2017 年 3 月 24 日

14SD102
Natsuki KINUGASA
衣笠 菜月

Supervisor: Professor Ryuji KOHNO
指導教官： 河野隆二 教授

Department of Physics, Electrical & Computer Engineering,
Graduate School of Engineering,
Yokohama National University
Kohno Laboratory
横浜国立大学大学院 工学府 物理情報工学専攻 河野研究室

Table of Contents

List of Figures

List of Tables

Acknowledgements

First of all, I would like to express the deepest appreciation to Professor Ryuji Kohno. Without his guidance and persistent help, this work would not have been possible. Moreover, I am grateful for the assistance given by Professor Fujinobu Takahashi. Advice and comments given by him have been a great help in carrying on with this work. I appreciate the constructive advices given by Professor Hiroshi Kumagai, Professor Hideki Ochiai, Professor Huan-Bang Li, Professor Chika Sugimoto, and Professor Keisuke Shima. I would also like to express my gratitude to Professor Takehiko Adachi and the members of his laboratory for their support for the experiment. I have had the support and encouragement of the members of Kohno laboratory and the secretaries as well. Finally, I would like to express my special thanks to my families and friends for their support.

Abstract

Ionosphere delay is the largest error factor for positioning using global navigation satellite system (GNSS), especially for single-frequency positioning. The electron density of ionosphere varies sometimes rapidly and locally due to the solar activity. The purpose of this work is to mitigate the ionospheric effect on single-frequency GNSS positioning. With the widespread of smartphones, the number of users of single-frequency positioning has been increasing explosively and its reliability is highly required. Therefore, this research can contribute to the reliable single-frequency GNSS positioning for huge number of users.

We proposed estimating the ionosphere delay in the process of the positioning calculation using single-frequency measurement with single epoch. The numerical evaluation conducted by measurements of American global positioning system (GPS) for selected five stations in Japan for both ionospheric quiet and stormy conditions during a period from 2013 to 2015. The correction effect on reducing the positioning error is higher than conventional correction method. However, it has an adverse effect on increasing the error rather than positioning without correction when the ionospheric effect on positioning is small.

The proposed ionosphere delay estimation method can be applied to not only GPS positioning but also multi-GNSS positioning, combining several satellite navigation systems. Currently, the operated satellite navigation systems are GPS, Russian GLONASS, European Galileo, Chinese BeiDou satellite system, Japanese quasi-zenith satellite system (QZSS), and Indian regional navigational satellite system (IRNSS). Using multi-GNSS positioning, the sufficient number of visible satellites is observable and the constellation is improved. Using selected satellite measurement which is suitable for positioning makes the positioning accuracy precisely, compared with using all visible satellites. In order to estimate the ionosphere delay more precisely for multi-GNSS positioning, we proposed the algorithm of selecting useful satellites by the residual ranging error of pseudorange measurement. From the performance evaluation conducted for GPS and Russian GLONASS positioning for ionospheric disturbed condition,

the satellite selection reduced the horizontal positioning error by maximum 20-60%. The ionosphere delay estimation with satellite selection reduced the error by maximum 60% at mid latitude region, compared with conventional one.

Chapter 1

Introduction

The signal of global navigation satellite system (GNSS) is refracted by the electrons when it propagates through the ionosphere. It is known that the ionospheric effect on radio wave is the largest propagation error. The thickness of ionosphere varies depending on the local time, the latitude, and the solar activity. The ionosphere generally behaves expectable in the calm domain. However, it is possible to fluctuate especially in the area near the equator and magnetic pole. That makes an electron density changes rapidly and can cause the scintillation and the fading on the signal [12].

The satellite of GNSS transmits two kinds of signals at 1.5 GHz band and at 1.2 GHz band. Dual-frequency receiver, which receives both signal, is used for the precise positioning for such as geodetic surveying. It can cancel the ionosphere delay which depends on the carrier frequency of signal. Single-frequency receiver, which receives only signal at 1.5 GHz, is equipped with smartphone, drone, car navigation, and some other devices. American global positioning system (GPS), Chinese BeiDou, and Japanese quasi-zenith satellite system (QZSS) provide the coefficients for ionosphere delay correction. The receiver corrects the measurement by applying them to the ionospheric model which was developed by Klobuchar in 1976 [5]. Feess and Stephens demonstrated that Klobuchar model can reduce 50% of ionospheric ranging error in 1987 [4]. Its correction effect for GPS positioning has been also widely studied [1] [2] [11]. Macalalad et al. showed that the percentage of error reduction using Klobuchar model was only 12 % at most examined for the ionospheric disturbed condition in Taiwan in 2013 [11]. Since the coefficients are uploaded every 24 hours, it is difficult to follow the rapid and local changes of ionosphere. For the ionosphere delay correction according to real-time ionospheric condition, it is necessary for single-frequency receiver to estimate the delay by itself.

With the widespread of the smartphone and tablet, the number of the users

of single-frequency receiver has been increased explosively. There are a lot of applications depending on the location information using GNSS for private use and also in industrial field. Therefore, the reliability of GNSS positioning using single-frequency receiver is required. The purpose of this work is to mitigate the ionospheric effect for huge number of users of single-frequency GNSS receiver.

In the process of positioning calculation, the estimated unknown parameters are three-dimensional position of receiver and receiver clock offset. Then, the number of visible satellites needs four at least. For GPS positioning, the number of visible satellites is usually between five and seven. Thus, we propose estimating the ionosphere delay in the process of positioning calculation by using more than five satellites. The estimation method is presented in [6]. The value of ionosphere delay included in the pseudorange measurement is different for each satellite. By representing the slant ionosphere delay by vertical delay and mapping function depending on the satellite elevation angle, the vertical delay can be estimated with receiver position and receiver clock offset. The performance of the proposed algorithm was evaluated by using the observation data at selected five stations in Japan. This thesis also compared its performance on ionospheric quiet and disturbed conditions for a period of 2013-2015. Its effect on reducing the horizontal positioning error is greater than that of conventional method using Klobuchar model especially in the daytime and during the disturbed ionospheric condition.

The satellite constellation viewed from the receiver highly affects the positioning accuracy. One of the solution to improve it is multi-GNSS positioning using several GNSS. Currently, the operated satellite navigation systems are GPS, Russian GLONASS, European Galileo, BeiDou, QZSS, and Indian IRNSS. However, each system has different correction method for the ionosphere delay. Then, the difference of ability of correction between systems is issue of combining different systems. The proposed estimation algorithm can be applied any single-GNSS positioning and multi-GNSS positioning.

For multi-GNSS positioning, sufficient number of visible satellites is observable. We considered positioning using only the satellite measurements with relatively small noise including multipath effect is much better than one with all visible satellites. We propose satellite selection algorithm for multi-GNSS positioning with ionosphere delay estimation.

This thesis consists of 7 chapters. Chapter 2 describes the background of positioning using GNSS. Chapter 3 describes the ionospheric effects on GNSS po-

sitioning and conventional correction method of ionosphere delay for different kinds of positioning. Chapter 4 describes the estimation method of ionosphere delay using single-frequency receiver with single epoch. Chapter 5 proposes mitigating the ionospheric effect on single-frequency single-GNSS positioning. Chapter 6 proposes mitigating the ionospheric effect on single-frequency multi-GNSS positioning with selection algorithm of satellites. Chapter 7 concludes this thesis. The relation between chapters can be found in Fig. 1.1.

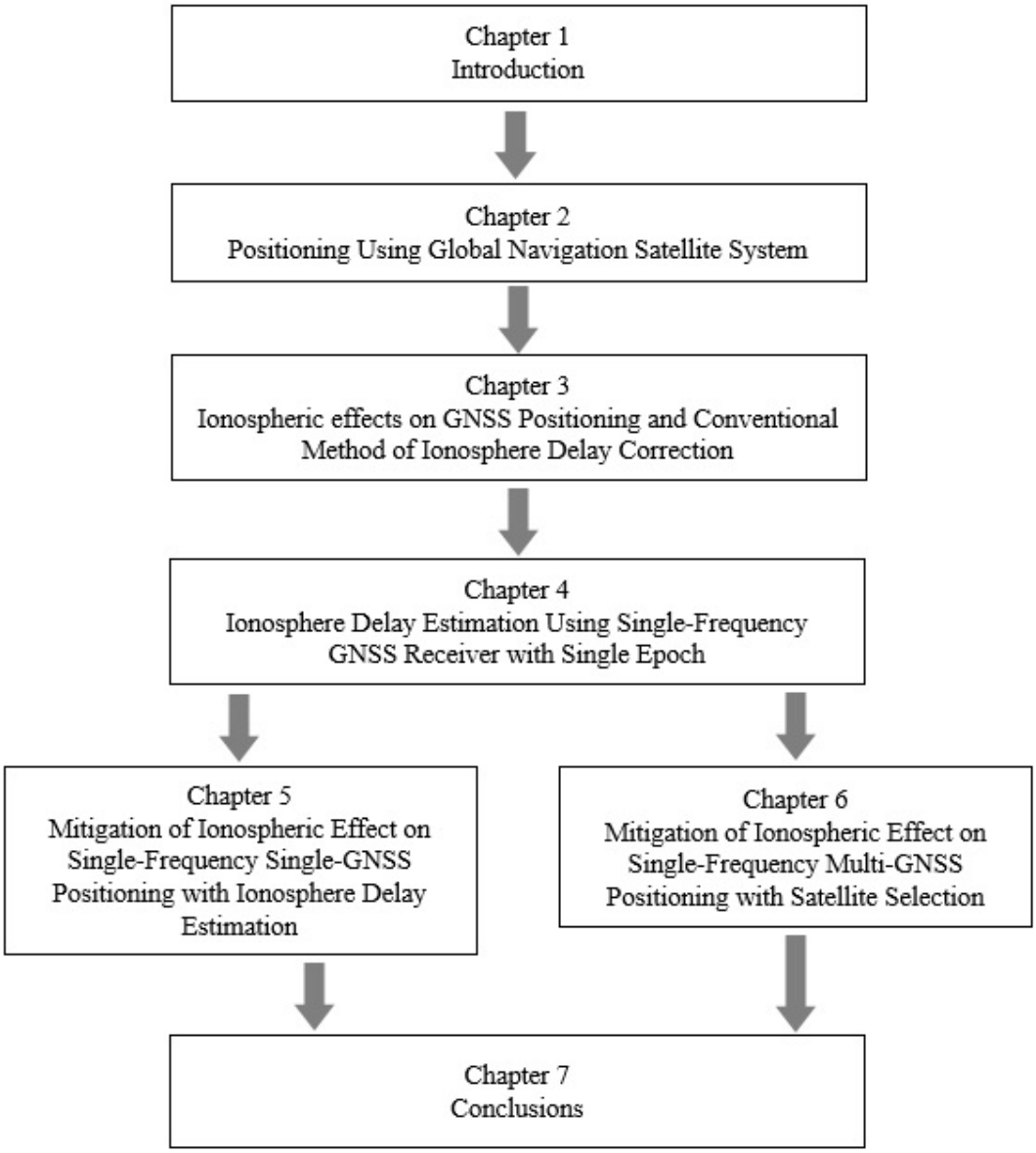

Figure 1.1 Flowchart of this thesis

Chapter 2

Positioning Using Global Navigation Satellite System

This chapter describes the background of positioning using global navigation satellite system (GNSS). Since several countries have developed the GNSS uniquely, there are some differences in the time system, the transmitted data, and etc. This also discusses the error factors for positioning and the positioning calculation method by numerical expressions.

2.1 GNSS

Global navigation satellite system has been operated by USA, Russia, European Union, Japan, China, and India. This section describes the differences between systems.

2.1.1 GNSS Developed by Each Country

Satellites of GPS have been launched and operated from 1970's by United States Department of Defense. The original objects were the navigation support and time synchronization. Since GPS is able to measure the baseline in the order of millimeter, it is used for geodetic survey. The residential use of GPS has been recognized for the people all over the world from 2000. Currently, there are easily more than a billion receivers in operation around the world. After Global positioning system (GPS) appears, four other navigation satellite systems have been launched: Russian GLONASS; European Galileo; Japanese QZSS; Chinese BeiDou; Indian IRNSS.

GPS, GLONASS, and Galileo, covering all over the world, are called global navigation satellite system (GNSS). For the complementation and compensation

of GNSS positioning, the regional navigation satellite system (RNSS) is operated by Japan, China, and India. Chinese BeiDou is the complex system of GNSS and RNSS. Three kinds of satellite orbit are operated: medium earth orbit (MEO); inclined geostationary orbit (IGSO); and geosynchronous orbit (GEO). MEO corresponds to GNSS and the rest correspond to RNSS.

System descriptions of GPS, GLONASS, and QZSS, used for the research of this thesis, are summarized in Table 2.1. The existing differences between systems cause the problem on multi-GNSS positioning, combining the different systems. These information were quoted from [18], [19], and [20].

Table 2.1 Comparison of GPS, GLONASS, and QZSS

	GPS	GLONASS	QZSS
Developed by	USA	Russia	Japan
Satellites	31	24	1
Inclination	55 degs	65 degs	43 degs
Orbital Planes	6	3	3
Orbital Cycle	11h 58m 2s	11h 15m 44s	11h 58m 2s
Altitude	20,180 km	19,100 km	35,786 km
Coordinate System	WGS84	PZ-90.02	JGS
Ephemeris	Orbit elements	ECEF coordinates of satellites	Orbit elements
Time system	GPS time	GLONASS time	QZSS time

2.1.2 GNSS Data

All essential information related to satellite ephemerides, satellite clocks, and message time marks is encoded in binary messages. GPS satellites transmit L1 civil signal navigation messages with a rate of 50 bps. The complete navigation message for GPS is transmitted within 12.5 min. Navigation messages consist of 24 frames of 30 sec durations. The most important and basic element of the navigation message is a subframe, which is 300 bit and lasts for 6 sec. The immediate orbital information relating to the transmitting satellite is encoded in subframes 1,2, and 3. The non-immediate information, such as almanac data for the system, is encoded in subframes 4 and 5. The subframe has a time mark, which is necessary to construct pseudorange measurements. QZSS orbital parameters are given in same format of GPS navigation message and use same algorithms to derive the satellite position.

A GLONASS navigation message consists of repeated superframes with durations of 2.5 min. Each superframe consists of 5 frames each with a duration of 30 sec. Each frame consists of 15 subframes, and each subframe has a duration of 2 sec. All essential data for the transmitting satellite are transmitted within each frame. Although GPS ephemerides are provided as a set of Keplerian osculating elements, GLONASS ephemerides are provided in tabular format. Each navigation message also provides the user with a time mark to pin down the satellite position to a specific moment of time.

2.2 Positioning Error Factors

The error factors of positioning are as follows.

(1) Receiver-related errors, including noise and hardware biases

(2) Satellite-related errors, including satellite clock error, satellite orbit errors, and satellite transmitter errors, including noise and biases

(3) Propagation errors in dispersive medium due to ionosphere

(4) Propagation errors in non-dispersive medium due to troposphere

(5) DOP arising from geometrical properties of the satellite constellation

(6) Multipath

Table 2.2 shows the error budget, quoted from [14]. The value of "Tropospheric delay" and "Ionospheric delay" denotes the remain error before correction. The tropospheric-, ionospheric-, and multipath-error are not expected because they depend on the atmospheric condition, the solar activity, and the environment around the receiver.

2.2.1 Receiver-Related Errors

The hardware biases, called inter-system biases (ISB), occur by the difference of delay in the receiver circuit of each GNSS. Then, it is necessary to estimate it for multi-GNSS positioning. The receiver noise includes the noises from antenna, amplifier, cables, and receiver, multi-access noise, and quantization noise.

Table 2.2 GNSS error budget

Error	Value for GPS (m)	Value for GLONASS (m)
Code phase noise	<1	<1
Orbits	≤1	≤10
Satellite clock	≤1.5	≤6
Tropospheric delay	2-25	2-25
Ionospheric delay	1.5-15	1.5-15
Multipath	0-10	0-10

2.2.2 Satellite-Related Errors

The broadcasted parameters of ephemeris and satellite clock are calculated by control segment of each GNSS. The control segment of each GNSS has the responsibility of keep the accuracy of broadcasted satellite position and satellite clock. Each satellite broadcasts its satellite clock offset between satellite clock and time system.

2.2.3 Ionosphere Delay

The signal of GNSS is refracted by the electrons when it propagates through the ionosphere. It is known that the ionospheric effect on radio wave is the largest propagation error. Ionosphere is the partial ionized domain that the atmosphere absorbs the ultraviolet rays. The thickness of ionosphere varies depending on the local time, the latitude, and the solar activity. The ionosphere generally behaves expectable in the calm domain. However, it is possible to fluctuate especially in the area near the equator and magnetic pole. That makes an electron density changes rapidly and can cause the scintillation and the fading on the signal [12].

Ionosphere is separated by four domains: D, E, F_1, and F_2 layers. In the D, E and F_1 layers, it is a state of the chemical equilibrium in generation and extinction of electron. An electron disappears because of the recombination of electron and ion. In the F_2 layer, ion and electron spread in the neutral atmosphere. That brings to the hydrostatic equilibrium. The distribution of ion and electron is converted from the chemical equilibrium to the diffusive equilibrium at around 300 km. At that height, the electron distribution is considered to be peak. The region above the ionosphere is called plasmasphere. Plasmasphere is the domain which is occupied by the plasma provided from the ionosphere. Both

satellites of GNSS and RNSS are located in the plasmasphere.

The thickness of ionosphere varies depending on the local time, the latitude, and the solar activity. The physical property of the ionosphere changes greatly in daytime and night. The electron density increases up to a peak in the day and decreases after that. The ionosphere generally behaves expectable in the calm domain. However, it is possible to fluctuate especially in the area near the equator and magnetic pole. That makes an electron density changes rapidly and can cause the scintillation and the fading on signal. The ionosphere delay is defined as

$$I = \frac{40.3TEC}{f^2} \tag{2–1}$$

where f is the signal frequency (Hz) and TEC is total electron content (TECU). TECU is the unit of TEC (1 TECU=$10^{16}el/m^2$). As shown in eq. (2–1), the ionosphere delay depends on the signal frequency and total electron content (TEC). In order to calculate the ionosphere delay, it is necessary for TEC to be estimated accurately. TEC is total number of the free electrons along the propagation path. TEC is also a valuable source of information for a great variety of ionospheric studies such as the space-weather, the ionospheric storm studies, and the earthquake studies, etc. TEC can be calculated by using the difference of the ionosphere delay of dual-frequency signals. When the dual-frequency measurements are treated, the inter-frequency biases of satellite and receiver always become a problem.

There are several methods of ionosphere delay correction for single point positioning. Their effect on mitigating the ionospheric effect is discussed in chapter 3.

2.2.4 Troposphere Delay

Signal of GNSS is also refracted by the lower part of atmosphere, which consists of dry air and water vapor. The troposphere is part of the Earth's atmosphere up to 16 km altitude. Troposphere delay cannot be estimated by GNSS measurement because it does not depend on the frequency of signal. Thus, the user of GNSS positioning needs to use the troposphere model. This work uses Saastamoinen model [12].

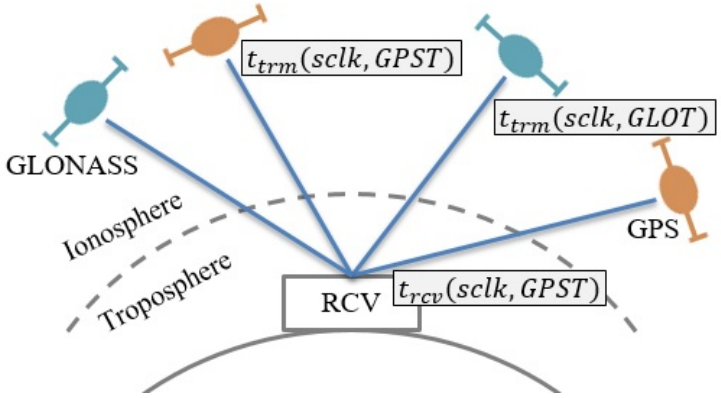

Figure 2.1 Satellite Positioning

2.2.5 Satellite Constellation

The accuracy of range measurement is limited by various errors due to the signal propagation in the atmosphere, the receiver, and the antennas and their surroundings. An error in positioning results from the errors in the range measurement multiplied by the geometry factor, discussed in section 2.3.4. Then, the errors in pseudorange, caused by atmospheric errors, propagate to create larger positioning errors. These positioning errors could be large when poor satellite geometry exists. That is why it is the extremely advantageous to have more satellites.

2.3 Positioning Calculation

This section defines the GNSS measurements and describes the algorithm of positioning calculation.

2.3.1 GNSS Measurements

Pseudorange measurement is calculated by multiplying the propagation time by speed of light c (m/sec). The propagation time is time difference between the received time t_{rcv} (sec) and transmitted time t_{trm} (sec) of signal which are measured by receiver clock ($rclk$) and satellite clock ($sclk$), respectively.

$$P \equiv c(t_{rcv}(rclk) - t_{trm}(sclk)) \tag{2–2}$$

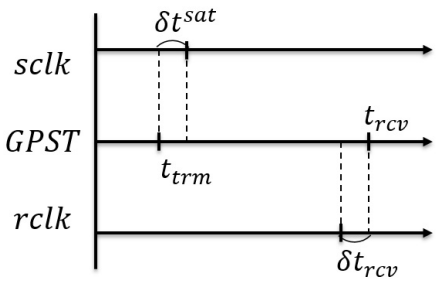

Figure 2.2 Relation between satellite clock and receiver clock

There is the receiver clock offset δt_{rcv} (sec) between receiver clock and GPS time ($GPST$).

$$t(rclk) = t(GPST) + \delta t_{rcv} \tag{2–3}$$

There is the satellite clock offset δt^{sat} (sec) between satellite clock and GPST or GLONASS time ($GLOT$).

$$t(sclk, GPS) \equiv t(GPST) + \delta t^{sat} \tag{2–4}$$

$$t(sclk, GLO) \equiv t(GLOT) + \delta t^{sat} \tag{2–5}$$

Satellite clock is not synchronized between satellites. Then, it is provided by each satellite in the navigation message. The relationships between GPS time and receiver clock offset and between GPS time and satellite clock offset are shown in Fig. 2.2.

Propagation distance includes the ionosphere delay I, troposphere delay T, and measurement noise (including multipath error) ϵ, in addition to the geometric distance between satellite and receiver r (All units are meter).

$$c(t_{rcv}(GPST) - t_{trm}(GPST)) = r + I + T + \epsilon \tag{2–6}$$

Thus, pseudorange measurement of GPS satellite is defined as follows.

$$P_{GPS} \equiv r + c(\delta t_{rcv} - \delta t^{sat}) + I + T + \epsilon \tag{2–7}$$

According to [15] and [14], there is the time difference δt_{sys} between GPST and GLOT (sec).

$$t(GPST) \equiv t(GLOT) + \delta t_{sys} \tag{2–8}$$

The transmitted time measured by GLONASS satellite clock is expressed as follows.

$$t_{trm}(sclk, GLO) = t(GPST) + \delta t^{sat} - \delta t_{sys} \tag{2–9}$$

Multi-GNSS positioning combining GPS and GLONASS needs to estimate it. Considering the time difference δt_{sys}, the pseudorange measurement of GLONASS is defined in the following equation.

$$P_{GLO} \equiv r + c(\delta t_{rcv} - \delta t_i^{sat} + \delta t_{sys}) + I + T + \epsilon \tag{2–10}$$

2.3.2 Positioning Calculation for single-GNSS

From eq. (2–7), the pseudorange measurement for single-GNSS positioning is given by

$$P_i = r_i + c(\delta t_{rcv} - \delta t_i^{sat}) + I_i + T_i + \epsilon_i \tag{2–11}$$

The parameters with index i is that of satellite i. The geometric distance r_i can be expressed as follows.

$$r_i = \sqrt{(x_i^{sat} - x_{rcv})^2 + (y_i^{sat} - y_{rcv})^2 + (z_i^{sat} - z_{rcv})^2} + \frac{\omega_e}{c}(x^{sat} y_{rcv} - y^{sat} x_{rcv}) \tag{2–12}$$

where $\begin{bmatrix} x_i^{sat} & y_i^{sat} & z_i^{sat} \end{bmatrix}$ and $\begin{bmatrix} x_{rcv} & y_{rcv} & z_{rcv} \end{bmatrix}$ are the earth-center earth-fixed (ECEF) coordinate of satellite i and receiver respectively (Units are meter). ω_e is the angular velocity of earth rotation (rad/s).

GNSS receiver usually estimates four unknown parameters: three dimensional coordinate of receiver $(x_{rcv}, y_{rcv}, z_{rcv})$ and receiver clock offset δt_{rcv}, in the process of usual positioning calculation by using measurements of four satellites at least. For the single-frequency positioning, satellite clock offset δt_i^{sat} is calculated by using clock correction parameters which are given in ephemeris. Troposphere delay model such as Saastamoinen and Hopfield is used for its correction [12]. Then, satellite clock offset δt_i^{sat} and troposphere delay T subtracted from pseudorange leave

$$\tilde{P}_i = r_i + c\delta t_{rcv}. \tag{2–13}$$

The variation of $\tilde{P}_i$ can be expressed by partial differentiation of $\tilde{P}_i$ and variation of each parameter.

$$\Delta\tilde{P}_i = \frac{\partial\tilde{P}_i}{\partial x_{rcv}}\Delta x_{rcv} + \frac{\partial\tilde{P}_i}{\partial y_{rcv}}\Delta y_{rcv} + \frac{\partial\tilde{P}_i}{\partial z_{rcv}}\Delta z_{rcv} + \frac{\partial\tilde{P}_i}{\partial s_r}\Delta s_r \tag{2–14}$$

where $s_r = c\delta t_{rcv}$. The partial differentiations of $\tilde{P}_i$ by each parameter are

$$\begin{aligned}
\frac{\partial \tilde{P}_i}{\partial x_{rcv}}\Delta x_{rcv} &= \frac{x_{rcv} - x_i^{sat}}{r}, \\
\frac{\partial \tilde{P}_i}{\partial y_{rcv}}\Delta y_{rcv} &= \frac{y_{rcv} - y_i^{sat}}{r}, \\
\frac{\partial \tilde{P}_i}{\partial z_{rcv}}\Delta z_{rcv} &= \frac{z_{rcv} - z_i^{sat}}{r}, \ and \\
\frac{\partial \tilde{P}_i}{\partial s_r}\Delta s_r &= 1.
\end{aligned}$$

Then, the parameters to be estimated are

$$\boldsymbol{X} = \begin{bmatrix} \Delta x_{rcv} & \Delta y_{rcv} & \Delta z_{rcv} & \Delta s_r \end{bmatrix}^{\mathrm{T}} \tag{2–15}$$

which are solved by the least square method as follows.

$$\boldsymbol{X} = \boldsymbol{G}^{-1}\boldsymbol{Y} \tag{2–16}$$

where $\boldsymbol{Y} = \left[\tilde{P}_1, \cdots, \tilde{P}_n\right]^T$. When n denotes the number of satellites, the geometry matrix becomes $n \times 4$ matrix.

$$\boldsymbol{G} = \begin{bmatrix} \boldsymbol{G_x} & \boldsymbol{G_y} & \boldsymbol{G_z} & \boldsymbol{G_{s_r}} \end{bmatrix} \tag{2–17}$$

where $\boldsymbol{G_x} \equiv \left[\frac{x_{rcv}-x_1^{sat}}{r_1}, \cdots, \frac{x_{rcv}-x_n^{sat}}{r_n}\right]^T$, $\boldsymbol{G_y} \equiv \left[\frac{y_{rcv}-y_1^{sat}}{r_1}, \cdots, \frac{y_{rcv}-y_n^{sat}}{r_n}\right]^T$, $\boldsymbol{G_z} \equiv \left[\frac{z_{rcv}-z_1^{sat}}{r_1}, \cdots, \frac{z_{rcv}-z_n^{sat}}{r_n}\right]^T$, and $\boldsymbol{G_{s_r}} \equiv [1, \cdots, 1]^T$.

2.3.3 Positioning Calculation for Multi-GNSS

This section describes the algorithm of multi-GNSS positioning combining GPS and GLONASS. The pseudorange measurement of GPS satellite is same as eq. (2–11). From eq. (2–10), the pseudorange measurement of GLONASS satellite is given by

$$P_i = r_i + c(\delta t_{rcv} - \delta t_i^{sat} + \delta t_{sys}) + I_i + T_i + \epsilon_i \tag{2–18}$$

The satellite clock offset δt_i^{sat} and troposphere delay T subtracted from pseudorange leave

$$\tilde{P}_i = r_i + c\delta t_{rcv} + c\delta t_{sys}. \tag{2–19}$$

The variation of $\tilde{P}_i$ can be expressed by partial differentiation of $\tilde{P}_i$ and variation of each parameter.

$$\Delta\tilde{P}_i = \frac{\partial\tilde{P}_i}{\partial x_{rcv}}\Delta x_{rcv} + \frac{\partial\tilde{P}_i}{\partial y_{rcv}}\Delta y_{rcv} + \frac{\partial\tilde{P}_i}{\partial z_{rcv}}\Delta z_{rcv} + \frac{\partial\tilde{P}_i}{\partial s_r}\Delta s_r + \frac{\partial\tilde{P}_i}{\partial s_{sys}}\Delta s_{sys} \quad (2\text{–}20)$$

where $s_{sys} = c\delta t_{sys}$. The partial differentiations of $\tilde{P}_i$ by time difference between GPS and GLONASS is

$$\frac{\partial\tilde{P}_i}{\partial s_{sys}}\Delta s_{sys} = 1$$

Then, the parameters to be estimated are

$$\boldsymbol{X} = \begin{bmatrix} \Delta x_{rcv} & \Delta y_{rcv} & \Delta z_{rcv} & \Delta s_r & \Delta s_{sys} \end{bmatrix}^{\mathrm{T}} \quad (2\text{–}21)$$

which are solved by the least square method as follows.

$$\boldsymbol{X} = \boldsymbol{G}^{-1}\boldsymbol{Y} \quad (2\text{–}22)$$

When n denotes the number of satellites, the geometry matrix becomes $n \times 5$ matrix.

$$\boldsymbol{G} = \begin{bmatrix} \boldsymbol{G_x} & \boldsymbol{G_y} & \boldsymbol{G_z} & \boldsymbol{G_{s_r}} & \boldsymbol{G_{s_{sys}}} \end{bmatrix} \quad (2\text{–}23)$$

where $\boldsymbol{G_{s_{sys}}} \equiv [a, \cdots, a]^T$. a is 0 for GPS and 1 for GLONASS.

2.3.4 Geometrical Factors

Equations (2–16) and (2–22) incorporate measurement errors. Then, measurement model should be written as follows:

$$\boldsymbol{Y} = \boldsymbol{G}\boldsymbol{X} + \boldsymbol{B} + \boldsymbol{\epsilon}, \quad (2\text{–}24)$$

$$\boldsymbol{\epsilon} \sim N(0, \boldsymbol{R}) \quad (2\text{–}25)$$

where $\boldsymbol{Y}$ is vector of measurements $(n \times 1)$, $\boldsymbol{G}$ is geometry matrix $(n \times m)$, $\boldsymbol{X}$ is unknown state vector $(m \times 1)$, $\boldsymbol{B}$ is a vector of bias $(n \times 1)$, and $\boldsymbol{\epsilon}$ is a vector of measurement errors $(n \times 1)$. $\hat{\boldsymbol{X}}$ minimizes the following equation.

$$\| \boldsymbol{Y} - \boldsymbol{G}\hat{\boldsymbol{X}} \|^2 = (\boldsymbol{Y} - \boldsymbol{G}\hat{\boldsymbol{X}})^T(\boldsymbol{Y} - \boldsymbol{G}\hat{\boldsymbol{X}}) \quad (2\text{–}26)$$

The unique solution of this system is

$$\hat{\boldsymbol{X}} = (\boldsymbol{G}^T\boldsymbol{G})^{-1}\boldsymbol{G}^T\boldsymbol{Y}. \quad (2\text{–}27)$$

Estimation error caused by measurement errors is expressed by

$$\begin{aligned}\tilde{\boldsymbol{X}} &= \hat{\boldsymbol{X}} - \boldsymbol{X} \\ &= (\boldsymbol{G}^T\boldsymbol{G})^{-1}\boldsymbol{G}^T(\boldsymbol{G}\boldsymbol{X} + \boldsymbol{B} + \boldsymbol{\epsilon}) - \boldsymbol{X} \\ &= (\boldsymbol{G}^T\boldsymbol{G})^{-1}\boldsymbol{G}^T(\boldsymbol{B} + \boldsymbol{\epsilon}).\end{aligned} \tag{2–28}$$

Expectation value of $\tilde{\boldsymbol{X}}$ can be expressed as follows:

$$E[\tilde{\boldsymbol{X}}] = (\boldsymbol{G}^T\boldsymbol{G})^{-1}\boldsymbol{G}^T\boldsymbol{B}. \tag{2–29}$$

Covariance matrix of $\tilde{\boldsymbol{X}}$ is also expressed as follows:

$$\begin{aligned}cov[\tilde{\boldsymbol{X}}] = E[\tilde{\boldsymbol{X}}\tilde{\boldsymbol{X}}^T] &= E[(\boldsymbol{G}^T\boldsymbol{G})^{-1}\boldsymbol{G}^T(\boldsymbol{B} + \boldsymbol{\epsilon})(\boldsymbol{B} + \boldsymbol{\epsilon})^T\boldsymbol{G}(\boldsymbol{G}^T\boldsymbol{G})^{-1}] \\ &= (\boldsymbol{G}^T\boldsymbol{G})^{-1}\boldsymbol{G}^T cov[\boldsymbol{B} + \boldsymbol{\epsilon}]\boldsymbol{G}(\boldsymbol{G}^T\boldsymbol{G})^{-1}\end{aligned} \tag{2–30}$$

When all components of the measurement covariance matrix are uncorrelated and have equal variances,

$$cov[\boldsymbol{B} + \boldsymbol{\epsilon}] = \sigma^2\boldsymbol{I} \tag{2–31}$$

where $\boldsymbol{I}$ is the identity matrix. Thus, equation (2–30) becomes

$$cov[\tilde{\boldsymbol{X}}] = \sigma^2(\boldsymbol{G}^T\boldsymbol{G})^{-1} \triangleq \sigma^2\boldsymbol{D}. \tag{2–32}$$

The value of $E[\tilde{\boldsymbol{X}}]$ and $cov[\tilde{\boldsymbol{X}}]$ describe the error propagation through geometry, which is called the dilution of precision (DOP). The diagonal elements of $cov[\tilde{\boldsymbol{X}}]$ define the DOP. The positional DOP (PDOP) is defined as:

$$PDOP = \sqrt{d_{11} + d_{22} + d_{33}} \tag{2–33}$$

where d_{ii} is an ith diagonal element of matrix $\boldsymbol{D}$. Then, three dimensional positioning error is estimated by

$$3D\ RMS\ positioning\ error = \sigma \cdot PDOP. \tag{2–34}$$

Figure 2.3 shows the variation of PDOP at station C on March 2015. Its calculation is based on the satellite constellation observed at station C on March 17, 2015. The detailed about data is explained in section 4.3 It indicates how the satellite constellation affects the error of single- and multi-GNSS positioning. It also shows that combining GPS and GLONASS can decrease the value of PDOP.

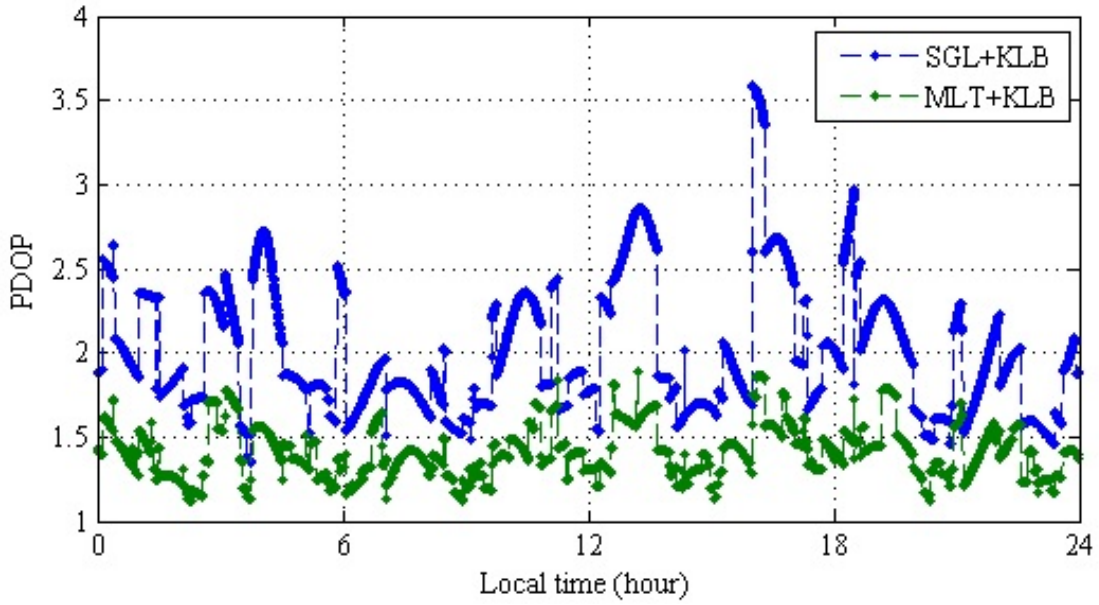

Figure 2.3 Variation of PDOP at station C on 17 March 2015

Chapter 3

Ionospheric Effects on GNSS Positioning and Conventional Method of Ionosphere Delay Correction

This chapter explains the ionospheric effects on GNSS positioning depending on the ionospheric condition. The effect of conventional correction method of ionosphere delay for each type of positioning is also discussed.

3.1 Ionospheric Effects on GNSS Measurements

This section describes the ionospheric effect on GNSS measurement, such as its dependence on ionospheric condition and latitude of observation point.

3.1.1 Dependence of Ionospheric Effects on Ionospheric Condition

Figure 3.1 compares the observed vertical TEC at station C during the ionospheric quiet and disturbed conditions. The data of "Quiet (mean)" means the average value of vertical TEC for eight ionospheric quiet days. The observed vertical TEC on quiet condition has the peak in daytime and gets small gradually, following the variance of ionospheric electron density. On disturbed condition, the magnitude of vertical TEC is large and it was observed that there were several peaks. The variance and magnitude of TEC on the disturbed condition is different from those on quiet condition. Thus, their effects on GNSS positioning are unrespectable.

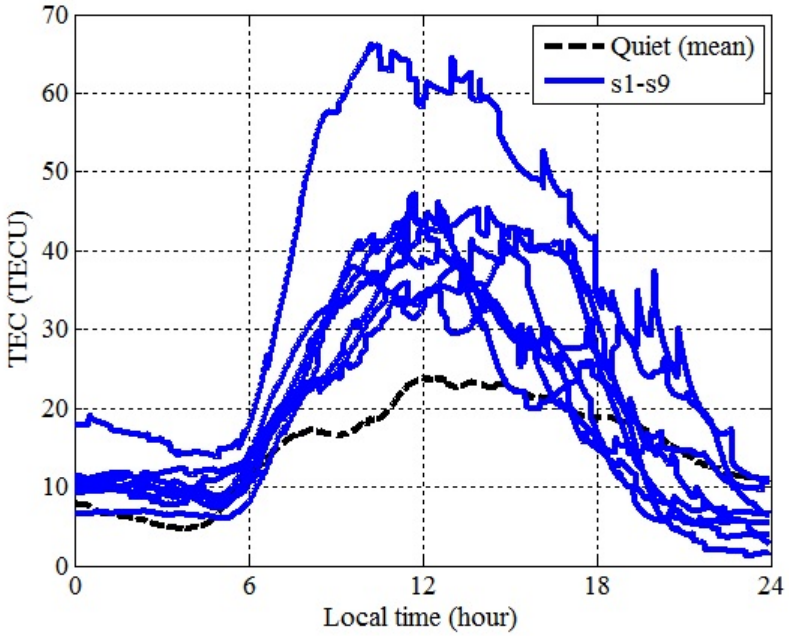

Figure 3.1 Dependence of vertical TEC observed at station C on ionospheric condition

3.1.2 Dependence of Ionospheric Effects on Latitude of Observation Point

Figure 3.2 compares the observed vertical TEC on 21 July 2014 during the ionospheric quiet condition at three stations in Japan. Station A is the northernmost and station D is the southernmost. The details of location of stations are described in Table TBL:station. On the quiet condition, there are no significant differences in the observed TEC value between stations.

Figure 3.3 also compares the observed vertical TEC on 9 November 2013 during the ionospheric disturbed condition at station A, C, and D. During the stormy condition, the dependence of the ionospheric effect on GNSS measurement is observed. The magnitude of vertical TEC observed at the southernmost station D is largest in daytime.

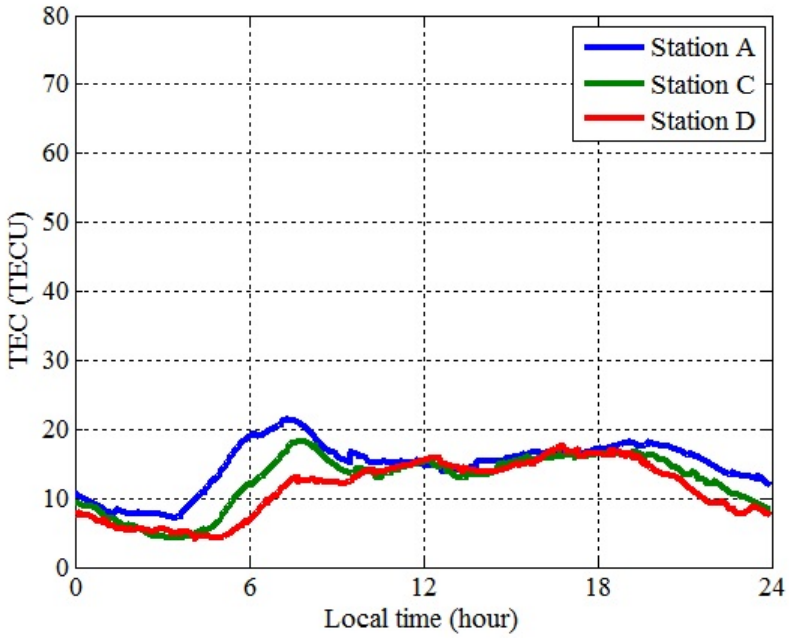

Figure 3.2 Dependence of vertical TEC observed during ionospheric quiet condition (21 July 2014) on the latitude of stations

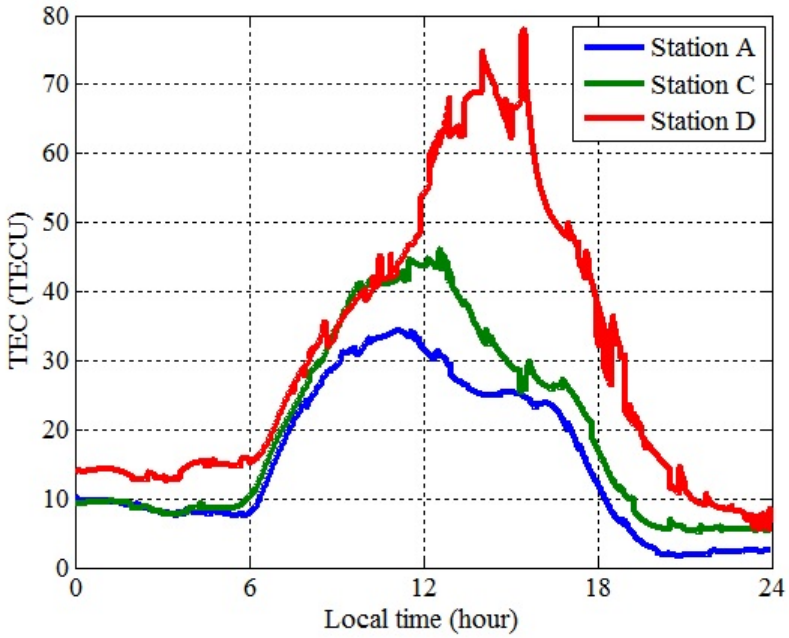

Figure 3.3 Dependence of vertical TEC observed during ionospheric disturbed condition (9 November 2013) on the latitude of stations

3.2 Conventional Ionosphere Delay Correction for Dual-Frequency Receiver

This section describes the conventional algorithm to correct the ionosphere delay for dual-frequency receiver.

3.2.1 Algorithm for Ionosphere-Free Technique

The ionosphere-free technique cancels the ionospheric effect on the measurement without TEC estimation by using pseudorange measurements.

This method generates the data free from the ionospheric effect by using the residual of dual-frequency measurements. The ionosphere delay can be separated from the pseudorange measurement in eq. (2–11) as follows.

$$P_{f_1} = P_{ion-free} + I_{f_1} + \epsilon_{f_1} \tag{3–1}$$

$$P_{f_2} = P_{ion-free} + I_{f_2} + \epsilon_{f_2} \tag{3–2}$$

From eq. (2–1), the ionosphere delay of L2 signal is expressed as follows.

$$I_{f_2} = \frac{f_1^2}{f_2^2} I_{f_1} \tag{3–3}$$

Then, the ionosphere delay-free pseudorange is defined as

$$P_{ion-free} = \frac{f_1^2}{f_1^2 - f_2^2} P_{f_1} - \frac{f_2^2}{f_1^2 - f_2^2} P_{f_2} + \epsilon \tag{3–4}$$

The error of satellite clock offset, receiver clock offset, and measurement noise remain in the ionosphere-free measurement.

3.2.2 Error Model

Unknown state vector of single-GNSS dual-frequency positioning for the least square method is defined as

$$\boldsymbol{X} = \begin{bmatrix} \Delta x_{rcv} & \Delta y_{rcv} & \Delta z_{rcv} & \Delta s_r \end{bmatrix}^{\mathrm{T}} \tag{3–5}$$

and one for multi-GNSS dual-frequency positioning is also defined as

$$\boldsymbol{X} = \begin{bmatrix} \Delta x_{rcv} & \Delta y_{rcv} & \Delta z_{rcv} & \Delta s_r & \Delta s_{sys} \end{bmatrix}^{\mathrm{T}} \tag{3–6}$$

The bias error of satellite j is given by

$$b_j = b^j_{orb} + b^j_{sclk} + b^j_{trop} \tag{3–7}$$

where b^j_{orb} and b^j_{sclk} are orbit error and clock error of satellite j. b^j_{trop} is modeling error of troposphere delay. All units are meter. Measurement noise is expressed as follows:

$$\epsilon_j = \frac{f_1^2}{f_1^2 - f_2^2}\epsilon_{1,j} - \frac{f_2^2}{f_1^2 - f_2^2}\epsilon_{2,j} \tag{3–8}$$

where $\epsilon_{i,j}$ is the measurement noise of signal of f_i Hz of satellite j. $\epsilon_j = 2.546 \cdots \epsilon_{1,j} - 1.546 \cdots \epsilon_{2,j}$ for GPS measurement and $\epsilon_j = 2.531 \cdots \epsilon_{1,j} - 1.531 \cdots \epsilon_{2,j}$ for GLONASS measurement.

$$\sqrt{2.546^2 + 1.546^2} \approx 3$$
$$\sqrt{2.531^2 + 1.531^2} \approx 3$$

Thus, the noise for dual-frequency positioning is approximately three times as large as one for single-frequency positioning. This indicates that the ionosphere-free technique can cancel the large bias due to the ionosphere delay, however the noise is added.

The section 3.3.2 compares the expectation value of positioing error using ionosphere free technique and with Klobuchar model.

3.2.3 Numerical Evaluation

Figures 3.4 compare the horizontal positioning error with ionosphere-free technique and without correction at station D on ionospheric disturbed condition. The result indicates that the ionosphere-free technique has highly effect of error reduction for dual-frequency positioning.

3.3 Conventional Ionosphere Delay Correction for Single-Frequency Receiver

Table 3.1 summarizes the ionosphere models used for ionospheric error compensation for each GNSS. GLONASS does not provide the compensation technique for single-frequency positioning. This section describes the algorithm to calculate the ionosphere delay by using Klobuchar model.

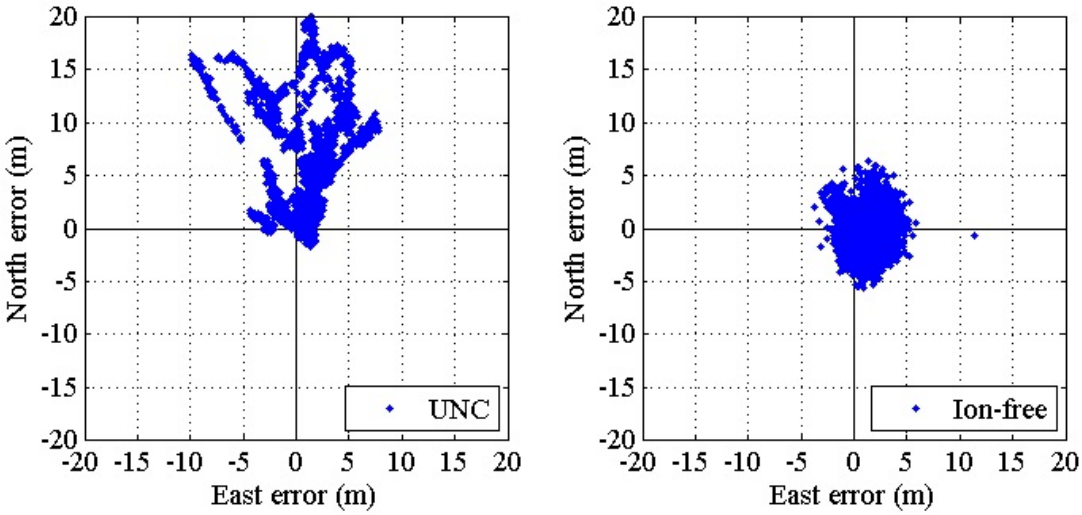

Figure 3.4 Positioning error without correction (left) and with ionosphere-free technique (right) at station D on disturbed condition (9 November 2013)

Table 3.1 Ionosphere models used for error compensation

GNSS	Ionosphere Model
GPS	Klobuchar
GLONASS	Not provided
Galileo	NeQuick
BeiDou	Klobuchar (planned)
QZSS	Klobuchar

3.3.1 Algorithm for Ionosphere Delay Calculation Using Klobuchar Model

Klobuchar developed the empirical ionosphere delay correction model, which is called Klobuchar model, for the user of single-frequency receiver in 1976 [5]. It is useful for single-frequency receiver to correct the delay for real-time.

This model represents the zenith delay as the constant value in nighttime and by the cosine function in daytime. The peak time of delay is set to 2 PM in local time anywhere on the earth. The correction coefficients ($\alpha_0, \alpha_1, \alpha_2, \alpha_3, \beta_0, \beta_1, \beta_2, \beta_3$) are given by each satellite of GPS and QZSS. They are updated once a day. It is supposed that this model halves root mean squares (rms) value of the positioning error caused by the ionosphere delay1.

The ionospheric correction model is given by

$$I = \left\{ \begin{array}{c} F \times [5.0 \times 10^{-9} + AMP \times (1 - \frac{x^2}{2} + \frac{x^4}{24}], |x| < 1.57 \\ F \times 5.0 \times 10^{-9}, |x| \geq 1.57) \end{array} \right\} \tag{3–9}$$

where $x = 2\pi(t - 50400)/PER$ and $F = 1.0 + 16.0(0.53 - EL)^3$. t is the local time when the signal reaches IPP. AMP means the amplitude of the cosine wave and is determined by the correction coefficients $(\alpha_0, \alpha_1, \alpha_2, \alpha_3)$.

$$AMP = \max \left\{ 0, \sum_{i=0}^{3} \alpha_i \phi_m^i \right\} \tag{3–10}$$

ϕ_m^i is the geomagnetic latitude. PER means the frequency of the cosine wave and is determined by the correction coefficients $(\beta_0, \beta_1, \beta_2, \beta_3)$.

$$PER = \max \left\{ 72000, \sum_{i=0}^{3} \beta_i \phi_m^i \right\} \tag{3–11}$$

3.3.2 Error Model

Unknown state vector of GNSS positioning with ionosphere delay correction using Klobuchar model is defined as follows:

$$\boldsymbol{X} = \left[\begin{array}{cccc} \Delta x_{rcv} & \Delta y_{rcv} & \Delta z_{rcv} & \Delta s_r \end{array} \right]^{\mathrm{T}}. \tag{3–12}$$

The bias of satellite j is given by

$$b_j = b_{orb}^j + b_{sclk}^j + b_{trop}^j + b_{ion}^j \tag{3–13}$$

where b_{ion}^j is modeling error of ionopshere delay (m). Measurement noise is expressed as follows:

$$\epsilon_j = \epsilon_{1,j}. \tag{3–14}$$

Figure 3.5 compares the expectation value of estimation error of GPS positioning with ionosphere-free technique and Klobuchar model, calculated by eq. (2–29). b_{orb} and b_{sclk} were set to the value of error budget in Table 2.2. b_{trop} was set to $0.6/\sin El$, which means that true value of vertical error is larger than modeling value by 0.6 m. Feess and Stephens demonstrated that Klobuchar model can reduce 50% of ionospheric ranging error in 1987 [4]. Then, b_{ion} was set to the correction value of Klobuchar model on March 17, 2015 at 15:00 (local time). The expectation value for single-frequency correction is always larger because of b_{ion} in eq. (3–13).

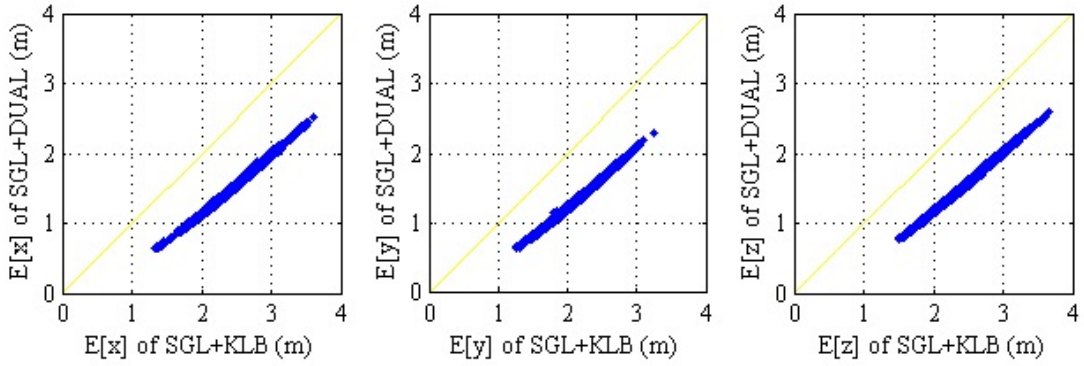

Figure 3.5 Comparison of the expectation value of estimation error of GPS positioning with ionosphere free technique and Klobuchar model

3.3.3 Numerical Evaluation

Figures 3.6 compare the horizontal positioning error with correction using Klobuchar model and without correction at station D on ionospheric disturbed condition. The result indicates that this method is not effective for error reduction.

Its correction effect for GPS positioning has been also widely studied [1] [2] [11]. Macalalad et al. showed that the percentage of error reduction using Klobuchar model was only 12 % at most examined for the ionospheric disturbed condition in Taiwan in 2013 [11]. Since the coefficients are uploaded every 24 hours, it is difficult to follow the rapid and local changes of ionosphere. For the ionosphere delay correction according to real-time ionospheric condition, it is necessary for single-frequency receiver to estimate the delay by itself.

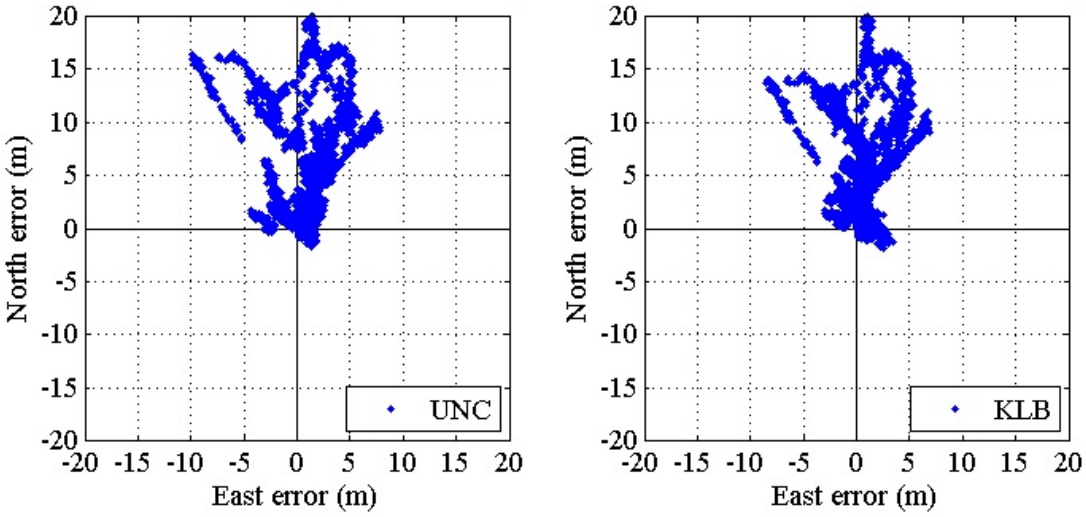

Figure 3.6 Positioning error with Klobuchar model and without correction on disturbed condition (9 November 2013)

Chapter 4

Ionosphere Delay Estimation Using Single-Frequency GNSS Receiver with Single Epoch

This chapter describes proposed algorithm to estimate ionosphere delay for single-frequency receiver using pseudorange measurements of single epoch. Secondly, it shows the theoretical evaluation of proposed algorithm, comparing with conventional Klobuchar model. Thirdly, it explained about GNSS data used for evaluation in this thesis and technique of evaluation. Finally, the appropriate parameter for ionospheric model used for the proposed algorithm is discussed.

4.1 Algorithm Description

Ionosphere delay which depends on the carrier frequency f (Hz) and the total electron content TEC (TECU) is expressed as eq. (2–1). Since TEC is the integral value of free electrons along the propagation path, slant value of TEC depends on the elevation angle of satellite. Plasma composed of ion and electrons is generated by solar energy. After dark, the electrons are recombined with ion and extinguished [13]. That is why the magnitude of TEC is large in daytime.

The pseudorange measurement is given by eq. (2–11). GNSS receiver usually estimates four unknown parameters: three dimensional coordinate of receiver and receiver clock offset, in the process of usual positioning calculation by using measurements of four satellites at least. In order to estimate the ionosphere delay included in measurement of each satellite by only pseudorange measurement, it is needed to be represented by small number of unknown parameters because the number of visible satellites is limited.

The slant delay I_{sl} (m) of each signal can be represented by the vertical delay I_{ver} (m) and the mapping function f_{map}. Mapping function converts vertical delay into slant delay as follows.

$$I_{sl} = f_{map} k I_{ver} \tag{4–1}$$

where $k = 1$ for measurement of GPS and $k = f_{L1}^2 / f_{R1}^2$ for measurement of GLONASS. f_{L1} and f_{R1} are the carrier frequency of signal of GPS and GLONASS (Hz), respectively. If the modeling error is small, the vertical delay can be estimated precisely.

4.1.1 Ionospheric Thin-Shell Model

This work applies the ionosphere thin shell model to the mapping function which is the simplest model, applied to Klobuchar model (see 3.3.1). This model supposes the ionosphere to be thin shell without a thickness, as shown in Fig. 4.1. Using the zenith angle χ at the intersection point of ionospheric thin shell and propagation path, the mapping function is given by

$$f_{map} = 1/\cos\chi \tag{4–2}$$

where

$$\chi = \arcsin\left(\frac{R_e \cos El}{R_e + H}\right) \tag{4–3}$$

R_e is the radius of earth, H is the altitude of thin shell of ionosphere (these units are meter), and El is elevation angle (radian). From Eqs. (4–1) through (4–3), the slant ionosphere delay can be expressed in the following equation.

$$I_{sl} = k\frac{1}{\cos\chi} I_{ver} \tag{4–4}$$

Fig. 4.2 shows the mapping function expressed in eq. (4–2) with various height H. When lower height is set, the ionosphere delay included in measurement of low-elevation satellite is assumed to be larger.

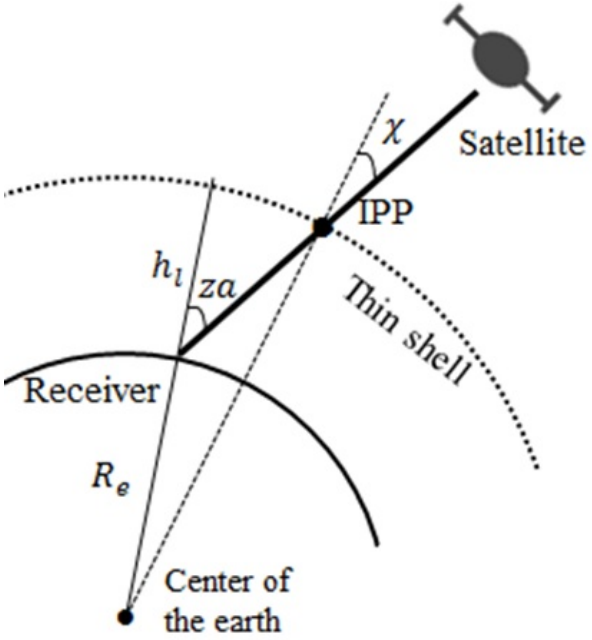

Figure 4.1 Ionospheric thin-shell model

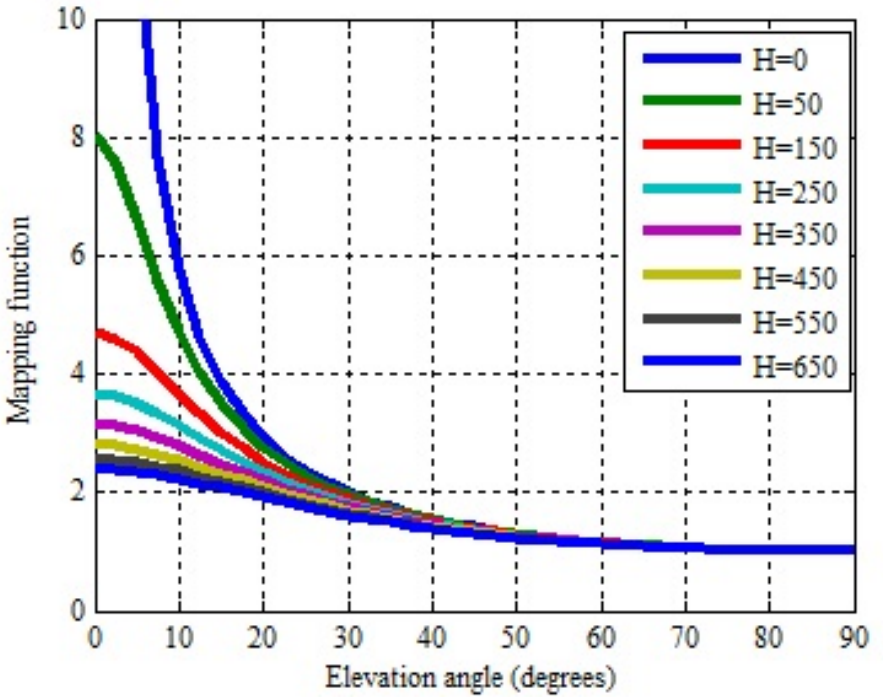

Figure 4.2 Mapping function of ionosphere thin-shell model

4.1.2 Ionosphere Delay Estimation Method

For single-frequency positioning, satellite clock offset is calculated by using clock correction parameters which are given in ephemeris. Troposphere delay model such as Saastamoinen and Hopfield is used for its correction [12]. Then, satellite clock offset δt_i^{sat} and troposphere delay T subtracted from pseudorange leave

$$\tilde{P}_i = r_i + c\delta t_{rcv} + \frac{k_i}{\cos\chi_i} I_{ver} \tag{4–5}$$

The variation of $\tilde{P}_i$ can be expressed by partial differentiation of $\tilde{P}_i$ and variation of each parameter.

$$\Delta\tilde{P}_i = \frac{\partial\tilde{P}_i}{\partial x_{rcv}}\Delta x_{rcv} + \frac{\partial\tilde{P}_i}{\partial y_{rcv}}\Delta y_{rcv} + \frac{\partial\tilde{P}_i}{\partial z_{rcv}}\Delta z_{rcv} + \frac{\partial\tilde{P}_i}{\partial s_r}\Delta s_r + \frac{\partial\tilde{P}_i}{\partial I_{ver}}\Delta I_{ver} \tag{4–6}$$

The partial differentiation of $\tilde{P}_i$ by ionosphere delay is

$$\frac{\partial\tilde{P}_i}{\partial I_{ver}} = \frac{k_i}{\cos\chi_i} \tag{4–7}$$

Then, the parameters to be estimated are

$$\boldsymbol{X} = \begin{bmatrix} \Delta x_{rcv} & \Delta y_{rcv} & \Delta z_{rcv} & \Delta s_r & \Delta I_{ver} \end{bmatrix}^{\mathrm{T}} \tag{4–8}$$

which are solved by the least square method as follows.

$$\boldsymbol{X} = \boldsymbol{G}^{-1}\boldsymbol{Y} \tag{4–9}$$

When n denotes the number of satellites, the geometry matrix becomes $n \times 5$ matrix.

$$\boldsymbol{G} = \begin{bmatrix} \boldsymbol{G_x} & \boldsymbol{G_y} & \boldsymbol{G_z} & \boldsymbol{G_{s_r}} & \boldsymbol{G_{ion}} \end{bmatrix} \tag{4–10}$$

where $\boldsymbol{G_{ion}} \equiv \left[\frac{k_i}{\cos\chi_1}, \cdots, \frac{k_i}{\cos\chi_n}\right]^T$.

For multi-GNSS positioning combining GPS and GLONASS, eq. (4–5) is written by

$$\tilde{P}_i = r_i + c\delta t_{rcv} + c\delta t_{sys} + \frac{k_i}{\cos\chi_i} I_{ver}. \tag{4–11}$$

The variation of $\tilde{P}_i$ can be expressed by partial differentiation of $\tilde{P}_i$ and variation of each parameter.

$$\Delta\tilde{P}_i = \frac{\partial\tilde{P}_i}{\partial x_{rcv}}\Delta x_{rcv} + \frac{\partial\tilde{P}_i}{\partial y_{rcv}}\Delta y_{rcv} + \frac{\partial\tilde{P}_i}{\partial z_{rcv}}\Delta z_{rcv} + \frac{\partial\tilde{P}_i}{\partial s_r}\Delta s_r + \frac{\partial\tilde{P}_i}{\partial s_{sys}}\Delta s_{sys} + \frac{\partial\tilde{P}_i}{\partial I_{ver}}\Delta I_{ver} \tag{4–12}$$

Then, the parameters to be estimated are

$$X = \begin{bmatrix} \Delta x_{rcv} & \Delta y_{rcv} & \Delta z_{rcv} & \Delta s_r & \Delta s_{sys} & \Delta I_{ver} \end{bmatrix}^{\mathrm{T}} \tag{4–13}$$

which are solved by the least square method as follows.

$$\boldsymbol{X} = \boldsymbol{G}^{-1}\boldsymbol{Y} \tag{4–14}$$

When n denotes the number of satellites, the geometry matrix becomes $n \times 6$ matrix.

$$\boldsymbol{G} = \begin{bmatrix} \boldsymbol{G_x} & \boldsymbol{G_y} & \boldsymbol{G_z} & \boldsymbol{G_{s_r}} & \boldsymbol{G_{s_{sys}}} & \boldsymbol{G_{ion}} \end{bmatrix} \tag{4–15}$$

In this way, time difference and ionosphere delay are estimated by the real time processing. However, the estimation of these parameters are affected by the ephemeris error, propagation modeling error, multipath, satellite constellation, etc. The estimated time difference δt_{sys} includes the hardware bias [15].

4.2 Theoretical Evaluation

Unknown state vectors for single-GNSS positioning and multi-GNSS positioning with ionosphere delay estimation are defined in eq. (4–8) and (4–13), respectively. The bias error and noise of satellite j are given by

$$b_j = b^j_{orb} + b^j_{sclk} + b^j_{trop} \tag{4–16}$$

and

$$\epsilon_j = \epsilon_{1,j}. \tag{4–17}$$

Figure 4.3 compares the expectation values of estimation errors of x_{rcv}, y_{rcv}, and z_{rcv} for GPS positioning with Klobuchar model and one with proposed ionosphere delay estimation. The values set to parameters are same in section 3.3.2. Figure 4.4 also compares them for GPS+GLONASS positioning. From these results, the expectation value of each parameter decreases by estimating the ionosphere delay.

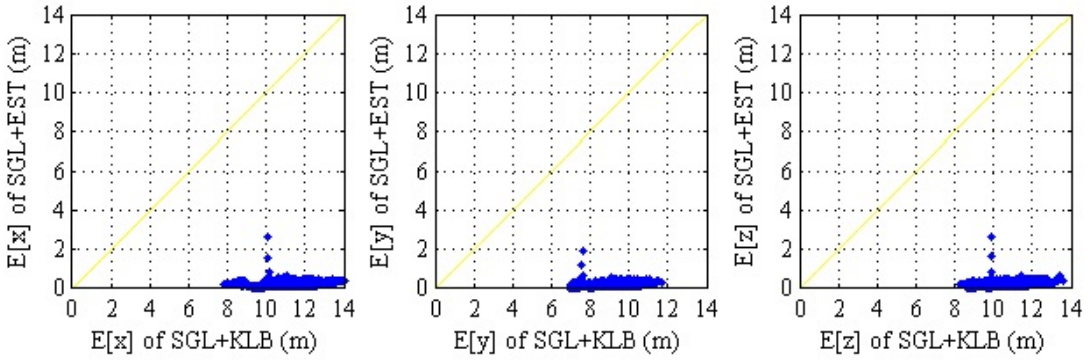

Figure 4.3 Comparison of expectation value of estimation error for GPS positioning

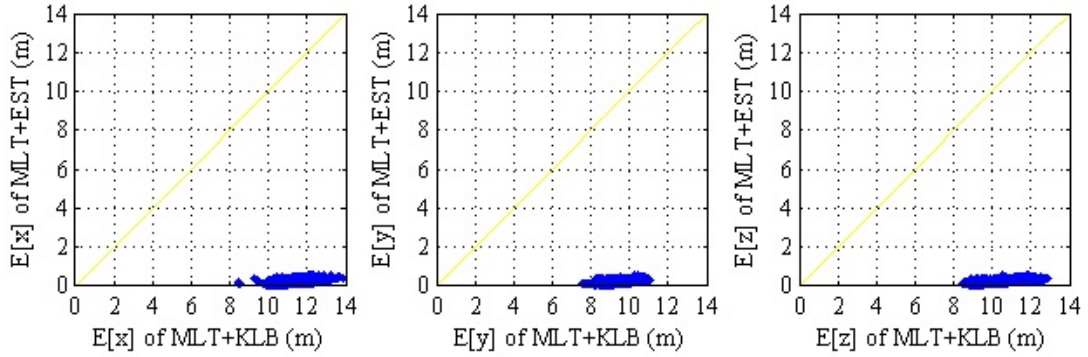

Figure 4.4 Comparison of expectation value of estimation error for GPS+GLONASS positioning

4.3 Numerical Evaluation

This section describes the data used for evaluation in this thesis and also technique of evaluation.

4.3.1 GNSS Data Used for Evaluation

For the performance evaluation of ionosphere delay correction in this work, the receiver independent exchange format (RINEX) files of GPS and GLONASS provided by GEONET which has been operated by Geospatial Information Authority of Japan (GSI) were used. The sampling interval of this file is 30 seconds. RINEX files consist of observation file and navigation file [21]. The observation file includes the measurements of pseudorange, carrier phase, signal strength, etc. The navigation file includes the navigation message, described in section 4.3.

We selected five stations in Japan which are located at geodetic latitude from 24.1 to 45.5 degrees north at intervals of about 5 degrees in order to evaluate the dependency of the performance on the geodetic latitude of the observation point. The details of the GEONET stations used for the evaluation is shown in Table 4.1. Station A is northernmost and station E is southernmost.

Table 4.1 Location of the GEONET stations used for the evaluation

Symbol	GEONET ID	Latitude (deg)	Longitude (deg)	Site Name
A	020848	45.5	142.0	Wakkanai 3
B	020923	40.1	140.0	Hachiryu
C	93032	35.4	139.7	Yokohama
D	960726	30.4	130.9	Minamitane
E	960751	24.1	123.8	Haterumajima

Table 4.2 describes the observation terms of both quiet and disturbed ionospheric conditions. As the sample of the quiet condition, the continuous observation data for eight days in July 2014 were used. Eight cases when the geomagnetic storms happened for a period from 2013 to 2015 were used as the sample of the disturbed condition. The indexes shown in Table 4.2 were obtained from WDC for Geomagnetism, Kyoto. The Kp index is the global geomagnetic storm index. Its range is from 0 to 9 where a value of 0 means that there is little geomagnetic activity and a value of 9 means extreme geomagnetic

storming [13]. The Dst index represents the axially symmetric disturbance magnetic field at the dipole equator on the earth surface. Negative variations in Dst are major disturbances when the decreases of geomagnetic fields are produced by the equatorial current system in the magnetosphere.

Table 4.2 List of observation days used for the evaluation with thier Dst index and Kp index

Symbol	Date (Local time)	Min. Dst index (nT)	Max. Kp index
s1	2/10/2013	-67	8-
s2	9/10/2013	-62	6-
s3	7/11/2013	-54	4
s4	9/11/2013	-81	5
s5	8/12/2013	-66	6
s6	19/2/2014	-112	6+
s7	28/2/2014	-99	5+
s8	17/3/2015	-223	8-
Quiet	18-25/7/2014	-13	3-

4.3.2 Software Development for Multi-GNSS Positioning

We developed the software for multi-GNSS positioning by MATLAB. The software mainly consists of three parts: Reading RINEX files; Satellite position Calculation; Positioning Calculation with ionosphere delay correction.

Positioning calculation used pseudorange measurements of 1.5 GHz signals of the visible GPS and GLONASS satellites for single epoch. The satellite position was interpolated with that given in ephemeris of RINEX navigation file. Saastamoinen model was employed for the troposphere delay model. The elevation mask was set to 10 degrees in this work.

4.3.3 Technique of Evaluation

Positioning error indicates the difference between true and the estimated position of receiver. It is calculated by expressing the estimated position in the east-north-up (ENU) coordinates using true receiver position as the origin. True coordinates of receiver is estimated and provided by GSI. The horizontal error is given by

$$Horizontal\ error = \sqrt{E^2 + N^2} \tag{4–18}$$

where E and N are the errors in the east and north directions respectively. The rms errors of each direction are labeled as $ERMS$ and $NRMS$. Horizontal rms error labeled as DRMSE is calculated as follows.

$$DRMSE = \sqrt{ERMSE^2 + NRMSE^2} \tag{4–19}$$

In order to describe the effect of each correction method on positioning error, the error reduction is calculated from the residual between the error without ionospheric correction e_{uncorr} and one with correction e_{corr}. Correction is effective when $e_{uncorr} - e_{corr} > 0$, while has an adverse effect when $e_{uncorr} - e_{corr} < 0$.

Figures 4.5 and 4.6 show the distribution of observed probability of GPS and GPS+GLONASS positioning, respectively. In order to see the effect of satellite constellation and ionospheric effect on positioning separately, we collected the statistics by the range of PDOP and horizontal positioning error without ionospheric correction e_{uncorr}. When e_{uncorr} is under 5 m, it is assumed that the ionospheric effect on positioning is highly unlikely. Figures suggest that the probability of occurrence of large value of e_{uncorr} is higher with higher latitude region. Fig. 4.6 also indicates the satellite constellation is improved by multi-GNSS positioning combining GPS and GLONASS.

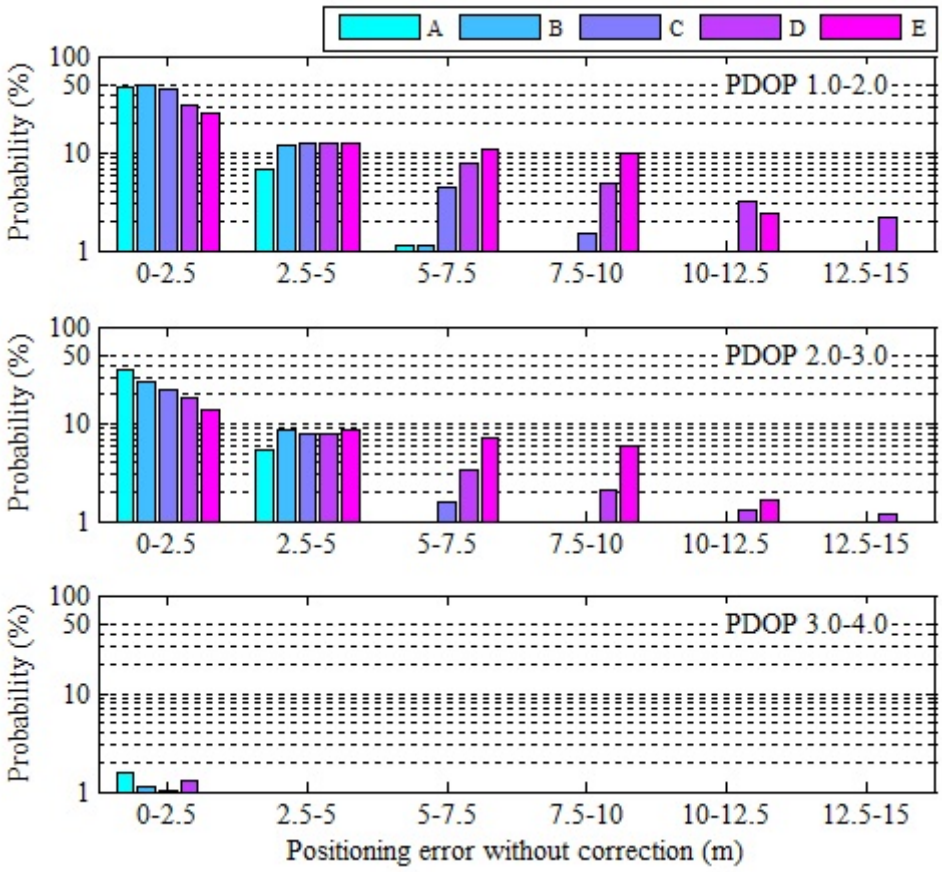

Figure 4.5 Distribution of observed probability of GPS positioning

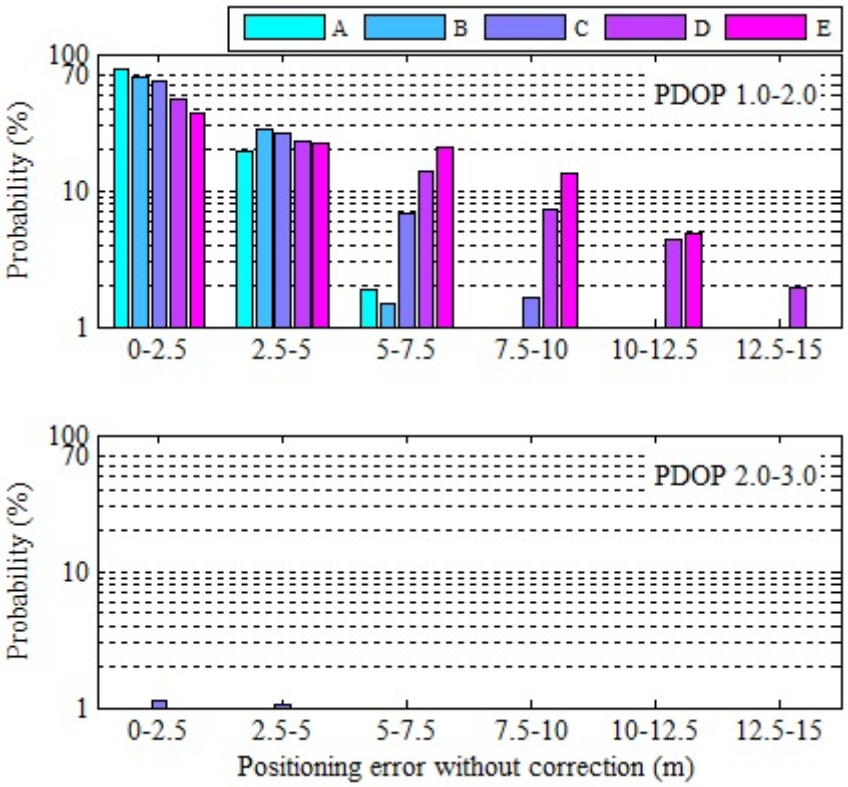

Figure 4.6 Distribution of observed probability of GPS+GLONASS positioning

4.4 Analysis of Appropriate Height of Ionospheric Thin-Shell Model

The peak of electron density in the ionosphere is about 350 km above from the surface of the earth [13]. Thus, the height of the ionospheric thin-shell H in eq. (4–3) is usually set to 350 km for the use of Klobuchar model, described in section 3.3.1. Appropriate height for the proposed ionosphere delay estimation using single-frequency pseudorange measurements should be discovered. The contents of this section is summarized in paper [7].

Figure 4.7 through 4.11 compare the DRMSE for GPS positioning when the height H was set to 0, 50, 150, 250, 350, 450, 550, and 650 km at selected five observation stations for ionospheric stormy period. The value of mapping function of ionospheric thin shell model depending on H is shown in Fig. 4.2

The result shows that there are no significant differences with various height H at every single stations when the ionospheric effect on positioning is small ($e_{uncorr} < 5$ m). However, setting lower height can reduce the DRMSE when $e_{uncorr} > 10$ m. This result indicates that the height of ionospheric thin-shell has an effect on positioning when the ionospheric effect is large. Then, It suggests that the ionospheric delay included in the measurement of low-elevation satellite is large. Thus, the height H was set to 50 km for the following numerical evaluation in this thesis.

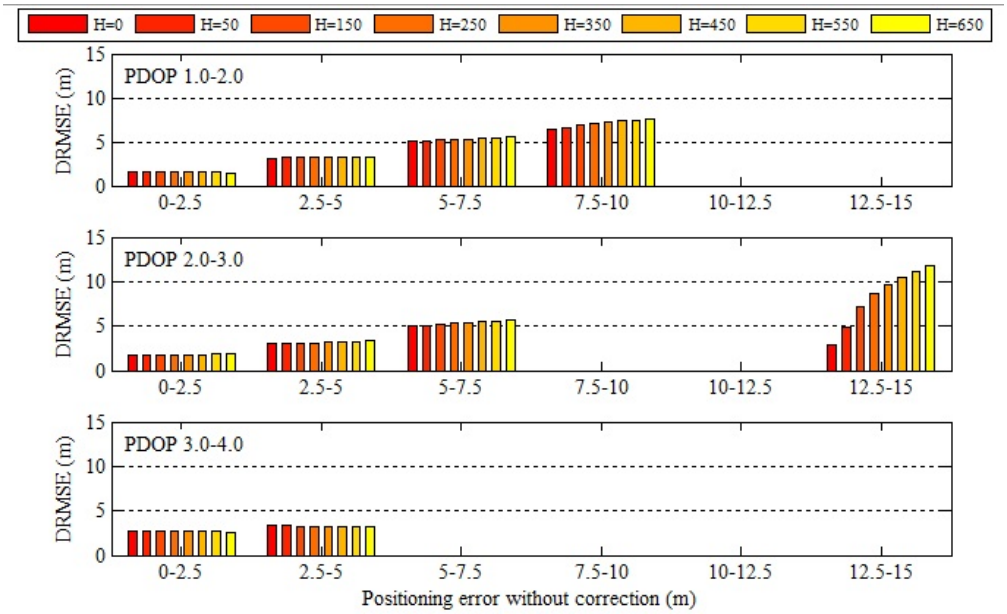

Figure 4.7 DRMSE for GPS positioning with various height of ionosphere at station A

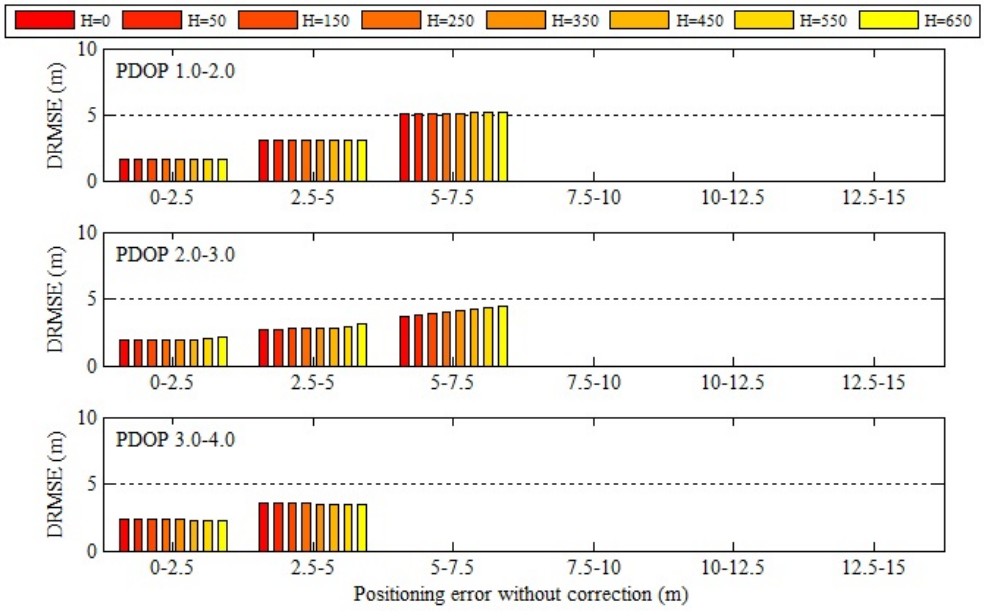

Figure 4.8 DRMSE for GPS positioning with various height of ionosphere at station B

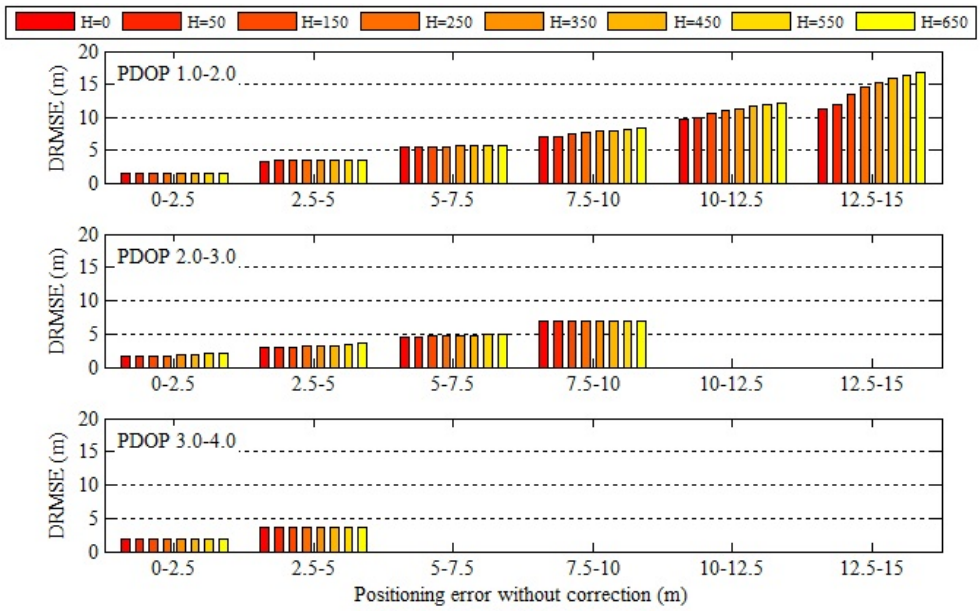

Figure 4.9 DRMSE for GPS positioning with various height of ionosphere at station C

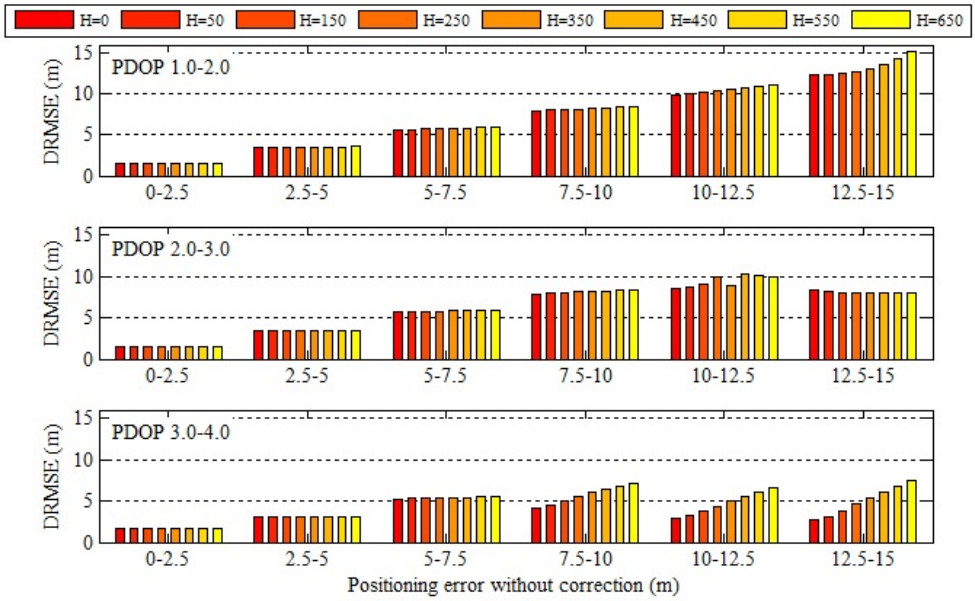

Figure 4.10 DRMSE for GPS positioning with various height of ionosphere at station D

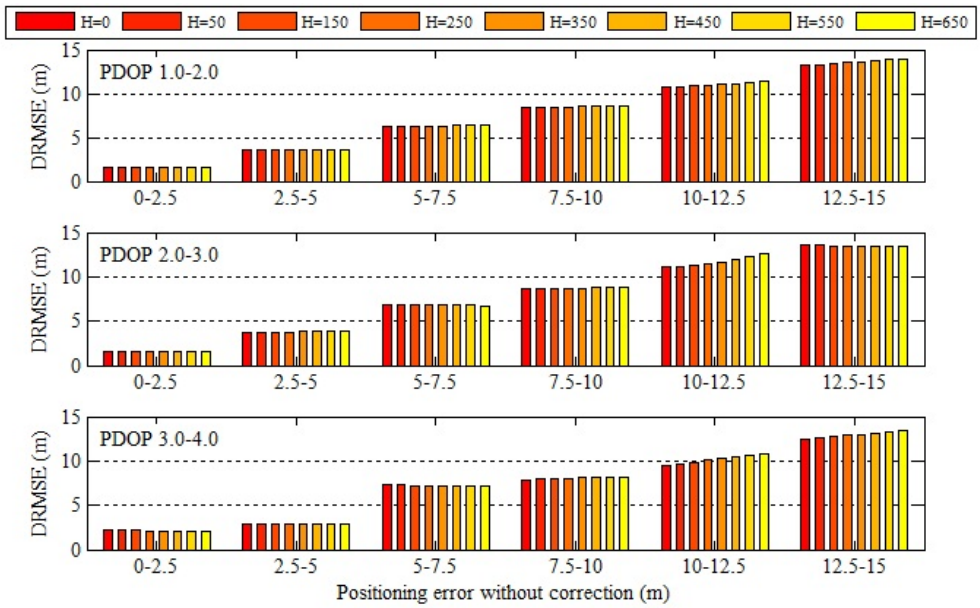

Figure 4.11 DRMSE for GPS positioning with various height of ionosphere at station E

Chapter 5

Mitigation of Ionospheric Effect on Single-Frequency Single-GNSS Positioning with Ionosphere Delay Estimation

We proposed estimation method of ionosphere delay using a single-frequency receiver and measurements of single epoch, described in Chapter 4. By representing the slant ionosphere delay by vertical delay and mapping function depending on the satellite elevation angle, the vertical delay can be estimated with receiver position and receiver clock offset. We discovered the appropriate height of ionosphere for Thin-shell model is 50 km.

This chapter firstly shows the result of numerical evaluation by using data observed at selected five stations in Japan for ionospheric disturbed conditions for a period of 2013-2015. Secondly, the drawback of proposal is discussed. The contents of this chapter is summarized in paper [6].

5.1 Performance Evaluation

Here, UNC, KLB, and EST imply the positioning without ionospheric correction, that with Klobuchar model, and that with ionosphere delay estimation. Figure 5.1 shows the horizontal positioning error without ionospheric correction (UNC). The measurements observed on 9 November, 2013 were used. The positioning error is over 5 m during 11:00-21:00 in local time when the ionospheric delay seems to be large.

Figures 5.2 and 5.3 also show the horizontal error reduction by conventional correction (KLB) and by proposed correction (EST), respectively. Although the

ionospheric effect on positioning is large in daytime, the correction effect of conventional method is not so higher, compared with that in nighttime. The result of proposed method indicates its effectiveness during 11:00-21:00.

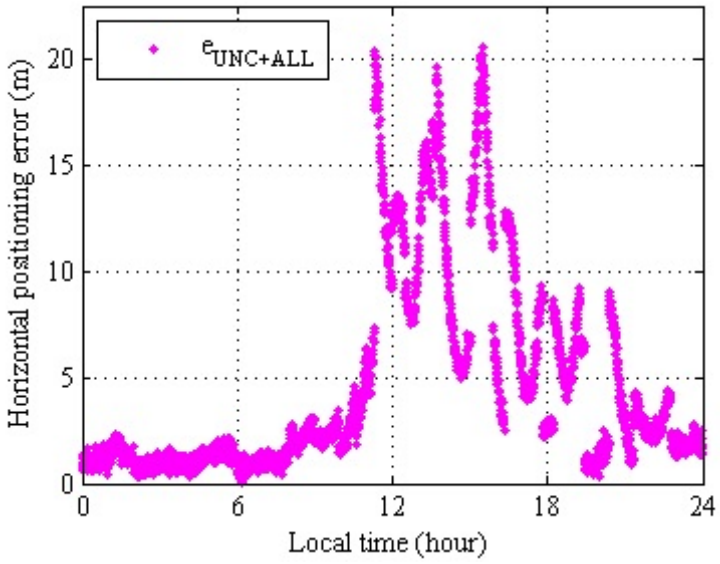

Figure 5.1 Horizontal positioning error of UNC at station D on 9 November, 2013

Figures 5.4 through 5.8 show the DRMSE for GPS positioning with ionosphere delay correction for stormy period at selected five stations in Japan. The results suggest that the effect of proposal on DRMSE reduction is almost equal or smaller than that of conventional method using Klobuchar model when the positioning error without correction e_{uncorr} is under 5 m. The result also shows indicates that its effect is larger with larger e_{uncorr}. At station A, EST reduces the DRMSE by 64%, compared with KLB. When e_{uncorr} is over 12.5 m, EST drastically reduces it to 5 m. At station B, EST reduces the DRMSE by 19%, compared with KLB. At station C, EST reduces the DRMSE by 13%, compared with KLB. At station D, EST reduces the DRMSE by 75%, compared with KLB. The proposed method is remarkably effective with e_{uncorr} >10 m and PDOP>3.0. At station E, EST reduces the DRMSE by 12%, compared with KLB. However, it was frequently observed in the result of station E that the proposal has an adverse effect. The reason of this is discussed in the following section.

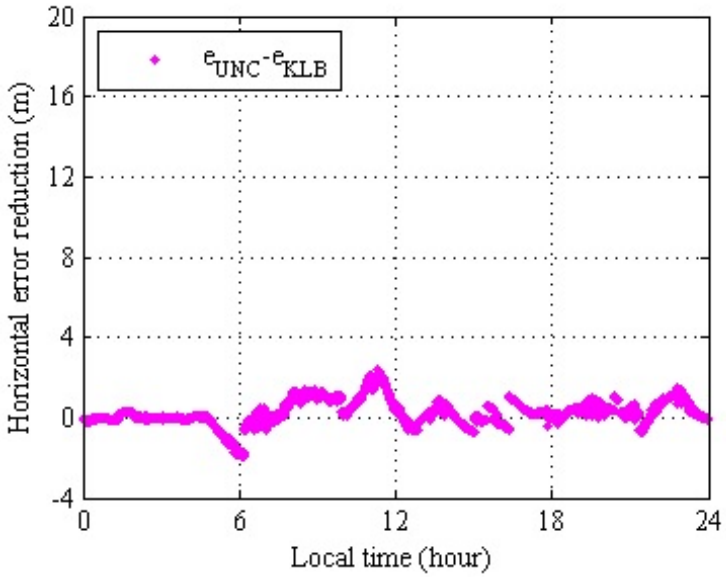

Figure 5.2 Horizontal error reduction by conventional correction (KLB) at station D on 9 November, 2013

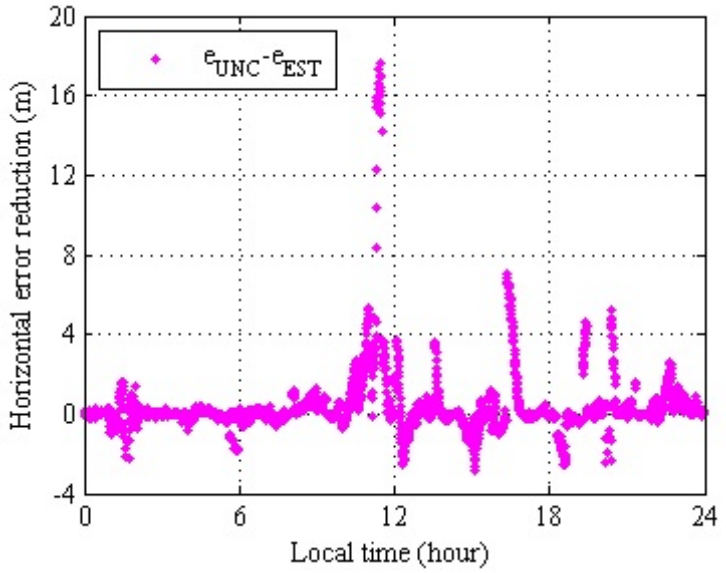

Figure 5.3 Horizontal error reduction by proposed correction (EST) at station D on 9 November, 2013

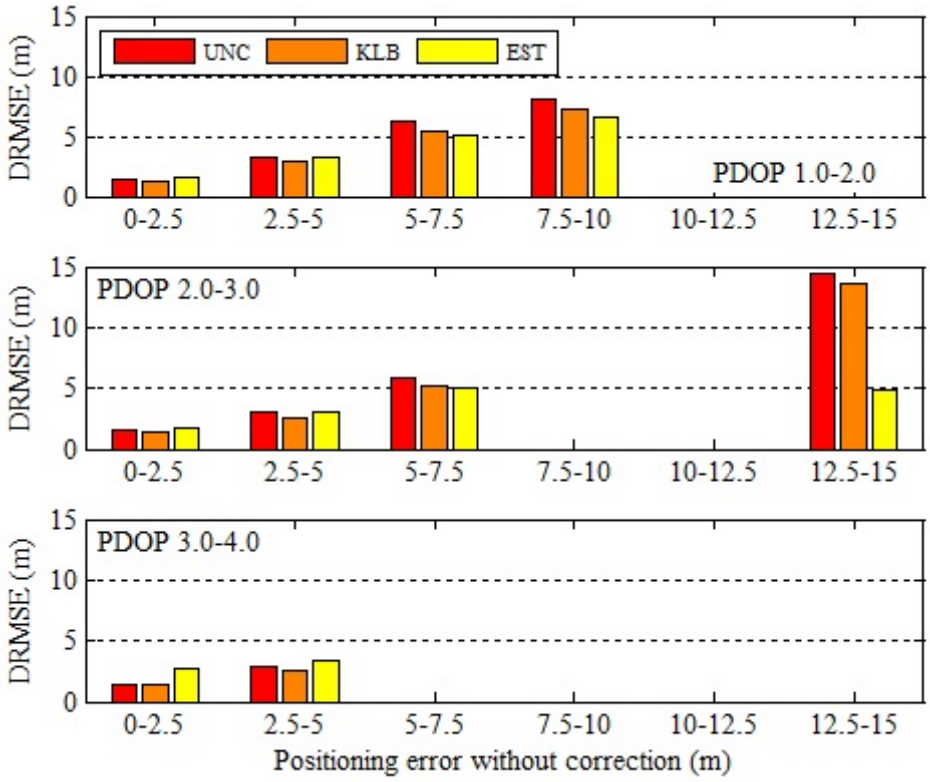

Figure 5.4 Comparison of DRMSE for GPS positioning with ionosphere delay correction for stormy period at station A

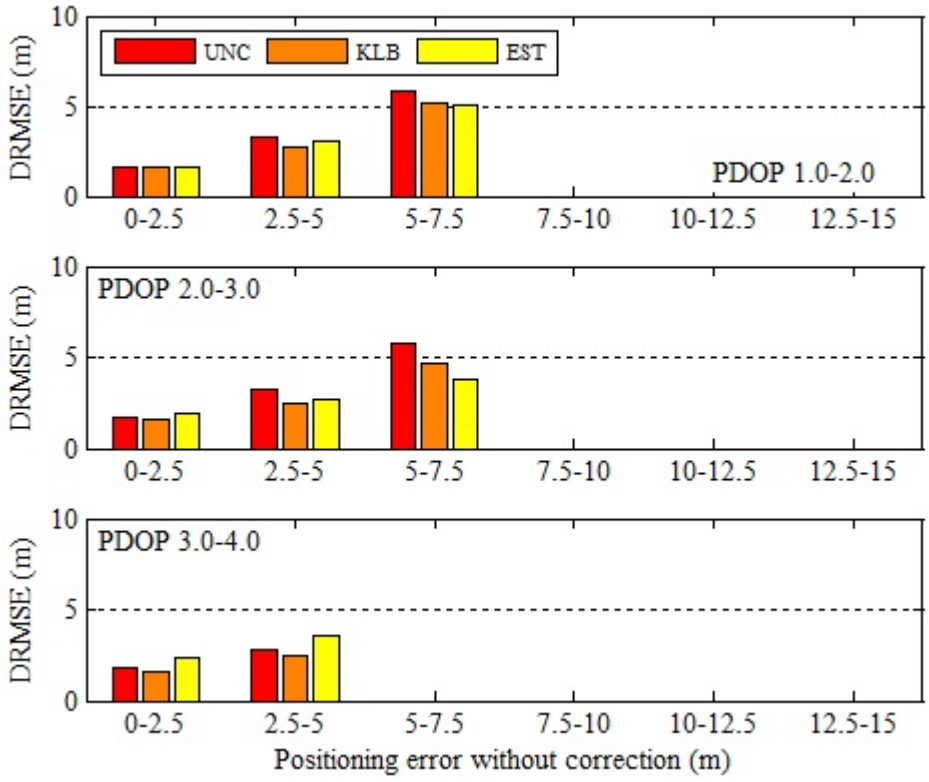

Figure 5.5 Comparison of DRMSE for GPS positioning with ionosphere delay correction for stormy period at station B

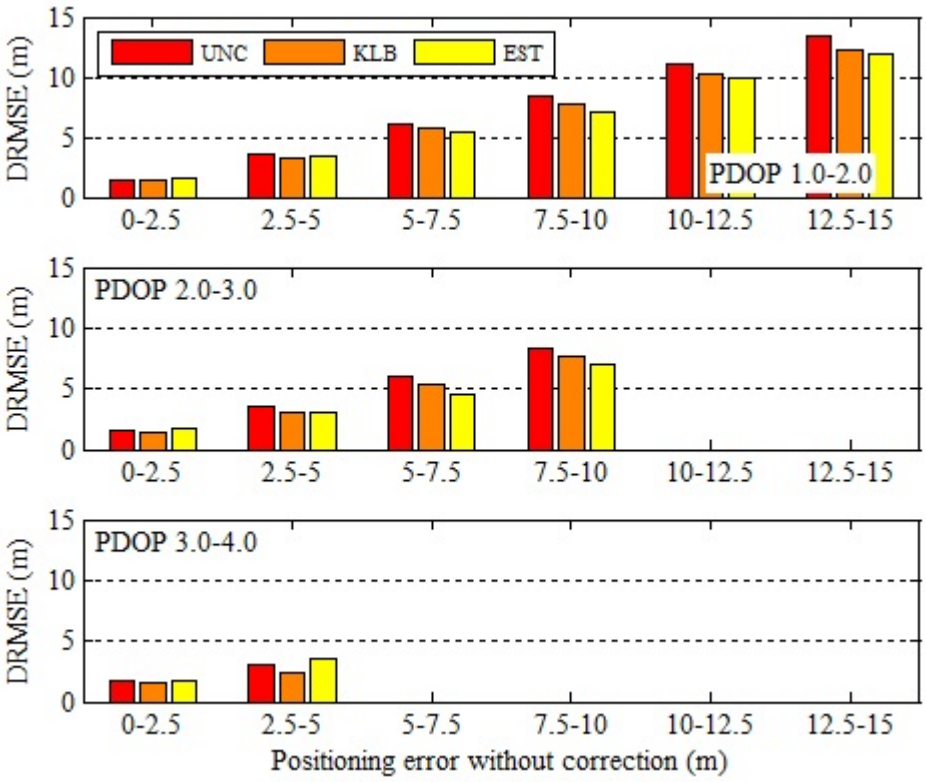

Figure 5.6 Comparison of DRMSE for GPS positioning with ionosphere delay correction for stormy period at station C

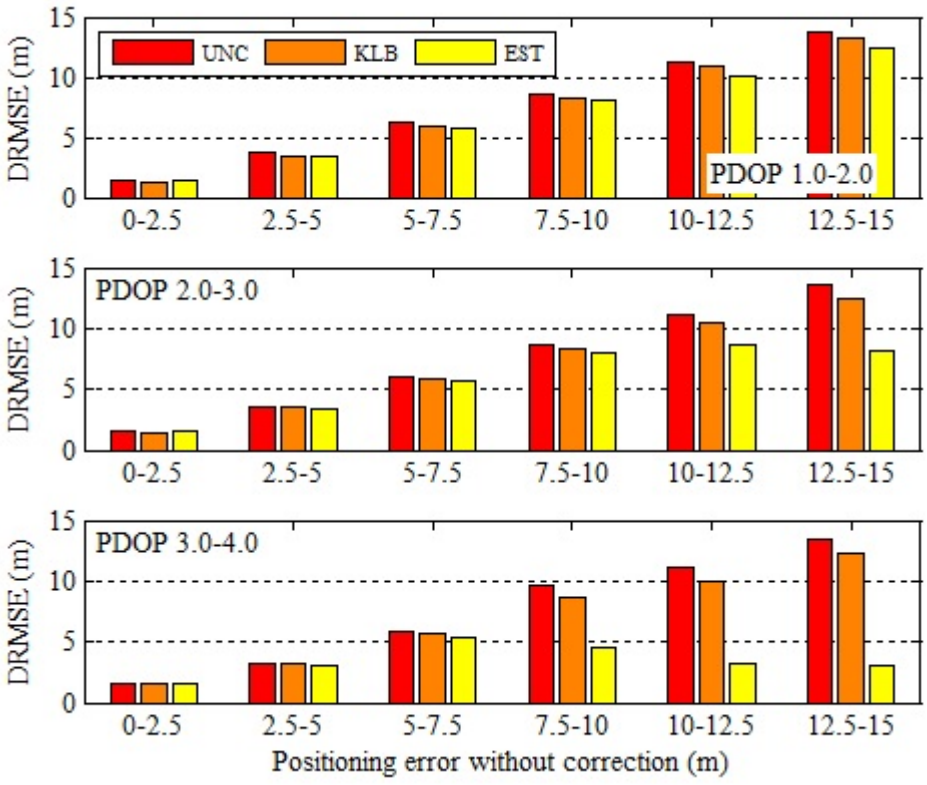

Figure 5.7 Comparison of DRMSE for GPS positioning with ionosphere delay correction for stormy period at station D

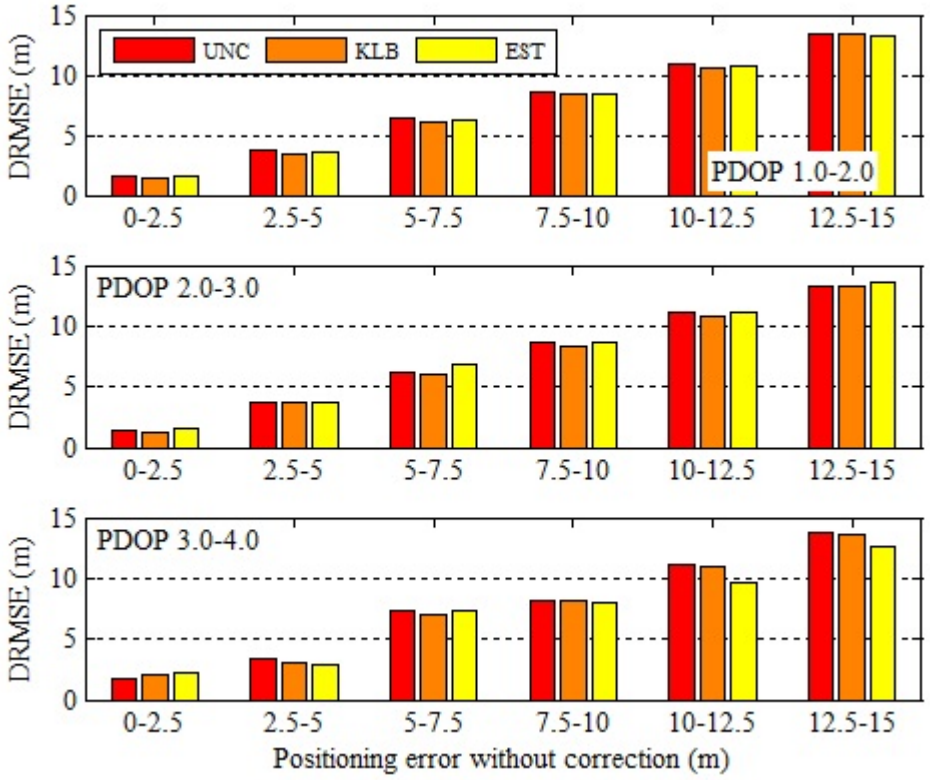

Figure 5.8 Comparison of DRMSE for GPS positioning with ionosphere delay correction for stormy period at station E

5.2 Drawback

There are differences of the correction effect of proposed ionosphere delay estimation method depending on the observation point, as shown in Figs. 5.4 through 5.8. At station E, the proposed correction is not so effective and an adverse effect was frequently observed. The ionospheric thin shell model introduced in this work assumes that the horizontal ionospheric electron density distribution is uniform and does not consider its dependence on the satellite azimuth angle, discussed in section 4.1.1. Signal of satellite which is located in south propagates through the region of high electron density the delay due to the ionospheric effect is definitely large. The ionospheric model, which considers its dependence on the azimuth angle, has been widely studied [9]. There is possibility to reduce the adverse effect by introducing one of these models especially for station nearer from equator.

5.2.1 Occurrence Condition of Degradation

Figure 5.9 compares the correction values of slant ionosphere delay included in QZSS pseudorange measurement generated by KLB and EST with true delay for station C for s6 in upper figure. The true delay which is labeled as TRUE was calculated from differences between dual-frequency pseudorange measurements. Residual between the correction value and the true delay, which denotes the ionospheric ranging error, is also shown in the lower figure. The value of EST varies along that of TRUE better than that of KLB except 18:00-21:20 in local time when the elevation of QZSS was under 10 degrees. Dependence of the ionospheric ranging error of QZSS on elevation angle for station C for s6 is shown in Fig. 5.10. The result also indicates that large error can be observed under 10 degrees in elevation angle. A similar tendency was seen among other GPS satellites as well. Then, the elevation angle should be set to 10 degrees at least if the number of visible satellites is sufficient. Thus, the proposed ionosphere delay estimation using measurement of single epoch needs to be applied for multi-GNSS positioning.

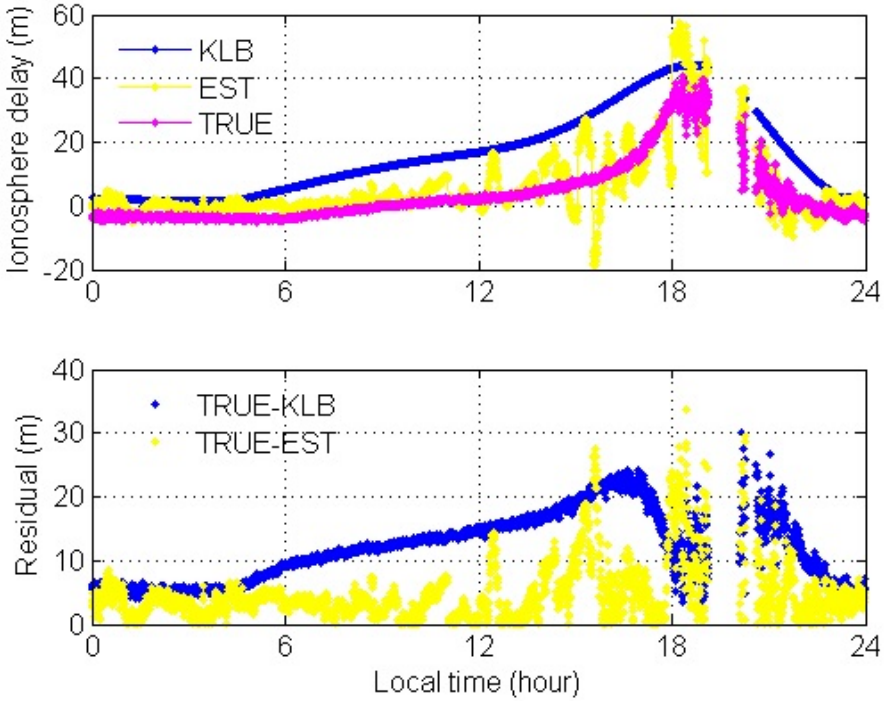

Figure 5.9 Comparison between correction values of slant ionosphere delay included in QZSS measurement generated by KLB and EST with true delay (TRUE) (Upper) and their residual (Lower) for station C on February 19, 2014

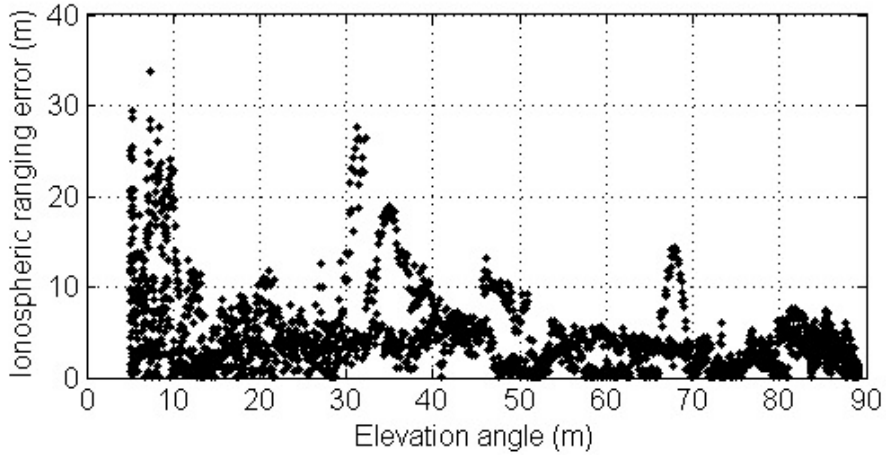

Figure 5.10 Dependence of ionospheric ranging error of QZSS on elevation angle for station C on February 19, 2014

Chapter 6

Mitigation of Ionospheric Effect on Single-Frequency Multi-GNSS Positioning with Satellite Selection

For the ionosphere delay correction according to real-time ionospheric condition, single-frequency receiver needs to estimate the delay by itself. We proposed estimation method of ionosphere delay by single-frequency receiver using GPS pseudorange measurements of single epoch [9] in Chapter 5. By representing the slant ionosphere delay by vertical delay and mapping function depending on the satellite elevation angle, the vertical delay is estimated with receiver position and receiver clock offset. An adverse effect was observed when ionospheric effect on positioning was originally small.

In this chapter, we apply the ionosphere delay estimation to multi-GNSS positioning which uses several GNSS together. Moreover, we propose using only the satellite measurements with relatively small error and noise including multipath effect which are positioning error factors. General smartphone can receive signals of GLONASS with those of GPS. Since sufficient number of visible satellites is observable by combining GPS and GLONASS, it does not necessarily use all those measurements. The contents of this chapter is summarized in paper [8].

6.1 Satellite Selection Algorithm

With multi-GNSS positioning, the sufficient number of satellites can be observed. Using selected measurements which is suitable for positioning is better than using all visible satellites. We propose using the absolute value of residual ranging error as the evaluation index for selecting the satellites used for

positioning. The residual ranging error is calculated by

$$\boldsymbol{A} = ||\boldsymbol{Y} - \boldsymbol{G}\hat{\boldsymbol{X}}||. \tag{6–1}$$

The residual ranging error includes positioning error, ephemeris error, satellite vehicle clock error, modeling error of ionosphere and troposphere, multipath effect, and measurement noise. The measurement with large residual ranging error makes the positioning accuracy worse. Thus, we propose eliminating such measurement of satellite i when its residual ranging error meets the following equation.

$$A_i > \mu + 2\sigma \tag{6–2}$$

where μ and σ are average and standard deviation (STD) of residual ranging errors of all visible satellites (Units are meter).

Figure 6.1 shows the flowchart of proposed positioning process. First process is positioning calculation with ionosphere delay estimation using the measurements of all visible satellites. Second one is calculation of the residual ranging error for all visible satellites using eq. (6–1). Third one is satellite selection by using the residual error as the evaluation index. Last one is positioning calculation with ionosphere delay estimation using the measurements of the selected satellite. The flowchart of satellite selection algorithm is shown in Fig. 6.2. If the residual error of satellite i does not meet eq. (6–2), its measurement is used for positioning. If it does, its measurement is not used basically. In order to prevent the position dilution of precision (PDOP) from remarkably deteriorating, the number of rest of satellites for each GNSS should be three or more. Even if it meets eq. (6–2), there is the case that its measurement is used for positioning.

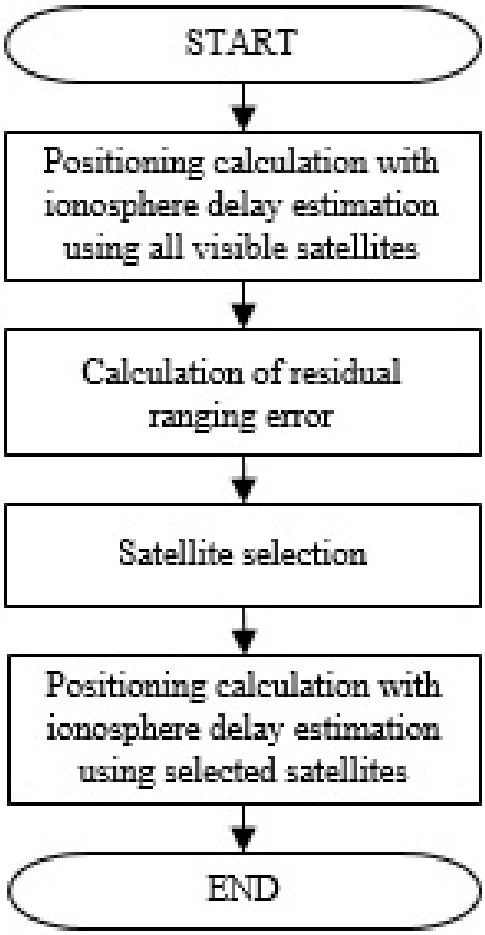

Figure 6.1 Flowchart of proposed positioning process

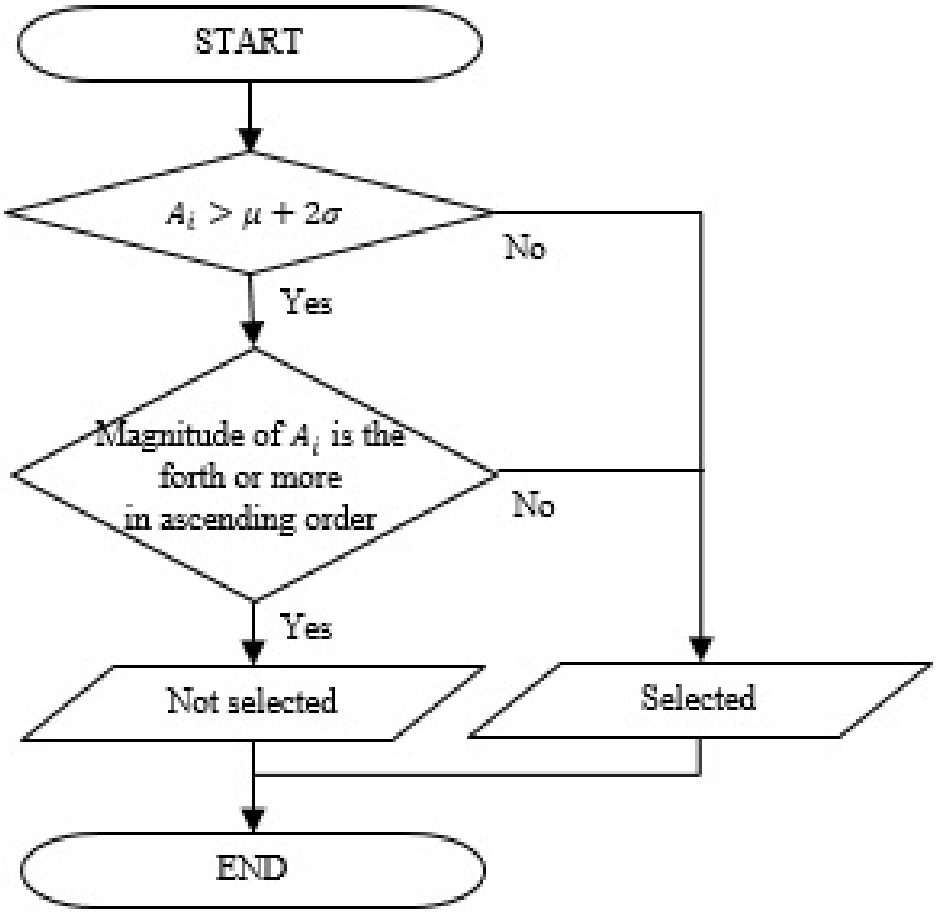

Figure 6.2 Flowchart of proposed satellite selection algorithm

6.2 Performance Evaluation

Performance evaluation was conducted by using measurements of GPS and GLONASS obtained at five stations in Japan for stormy period. Firstly, the evaluation for the effect of satellite selection on mitigation of positioning error is presented. Secondly, the evaluation for the effect of ionosphere delay correction using conventional method and proposed estimation method is presented.

6.2.1 Effect of Satellite Selection

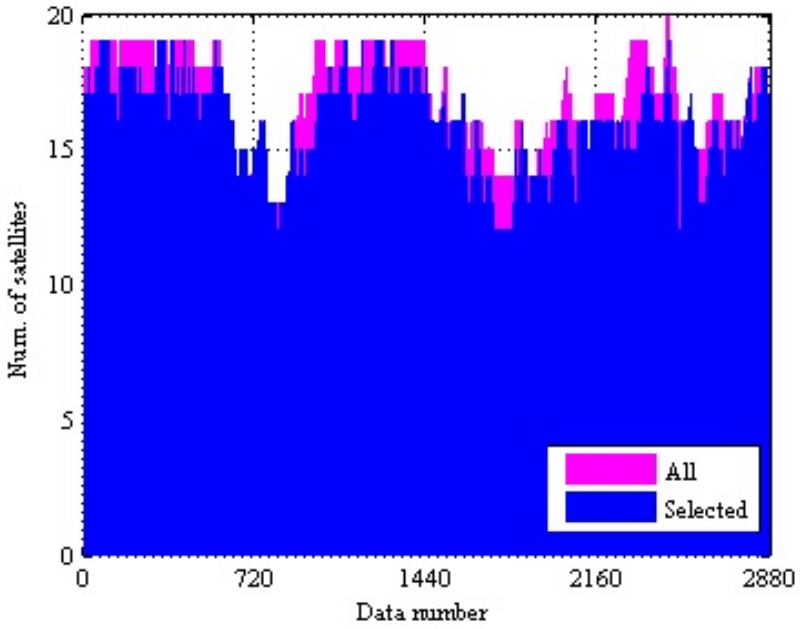

Figure 6.3 Number of satellites used for positioning observed at station D on 28 February, 2014

Figure 6.3 shows the number of satellites used for GPS+ GLONASS positioning at station D on 28 February 2014 as the example. The result labeled as "All" means the number of satellites whose elevation is 10 degrees or more. The result labeled as "Selected" means that of selected satellites with proposed selection algorithm. Proposed positioning calculation needs six satellites at least. Thus, the number of selected satellites is sufficient for positioning throughout the whole day. Table 6.1 summarizes the execution rate of removal of satellite measurements by selection algorithm.

Table 6.1 The execution rate of removal of satellite measurements by selection algorithm

Station	A	B	C	D	E
Rate (%)	95.9	95.6	94.9	95.6	97.2

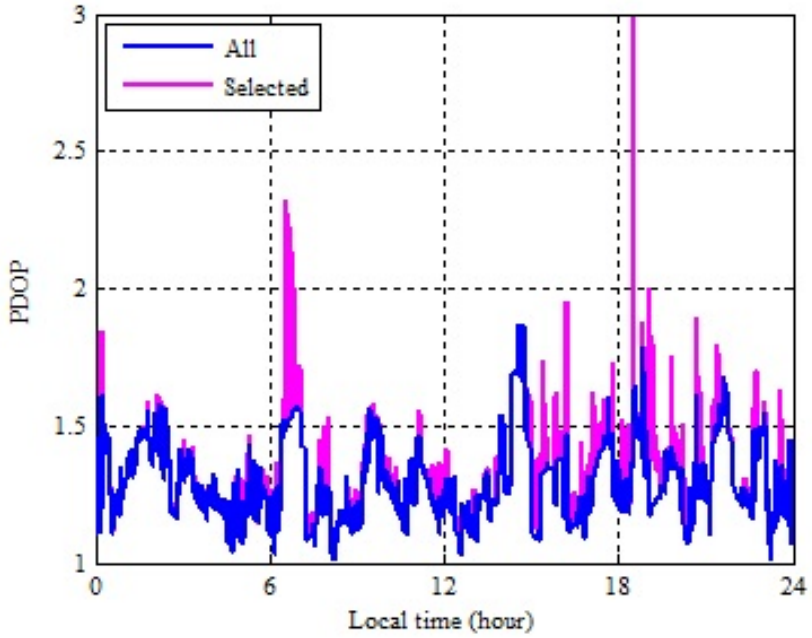

Figure 6.4 PDOP at station D on 28 February, 2014

Figure 6.4 compares the PDOP at station D on 28 February 2014 before and after selection. By combining GPS and GLONASS, PDOP was kept less than 3.0 throughout the whole day even if four satellites were removed from positioning calculation. This suggests that the proposed algorithm appropriately selected satellites without remarkably increasing PDOP.

Figures 6.5 through 6.9 show the DRMSE for GPS+GLONASS positioning with ionosphere delay estimation using all visible satellites or selected satellites for stomry period at five stations, respectively. This statistics is based on the value of PDOP after satellite selection. When the positioning error without correction is large, the correction effect on DRMSE reduction is large. The results of all stations suggest that the effectiveness of satellite selection is enlarged in the case of bad satellite constellation. At station A, proposed selection algorithm reduces the DRMSE by 30%. At station B, proposed selection algorithm reduces the DRMSE by 28%. At station C, proposed selection algorithm reduces the

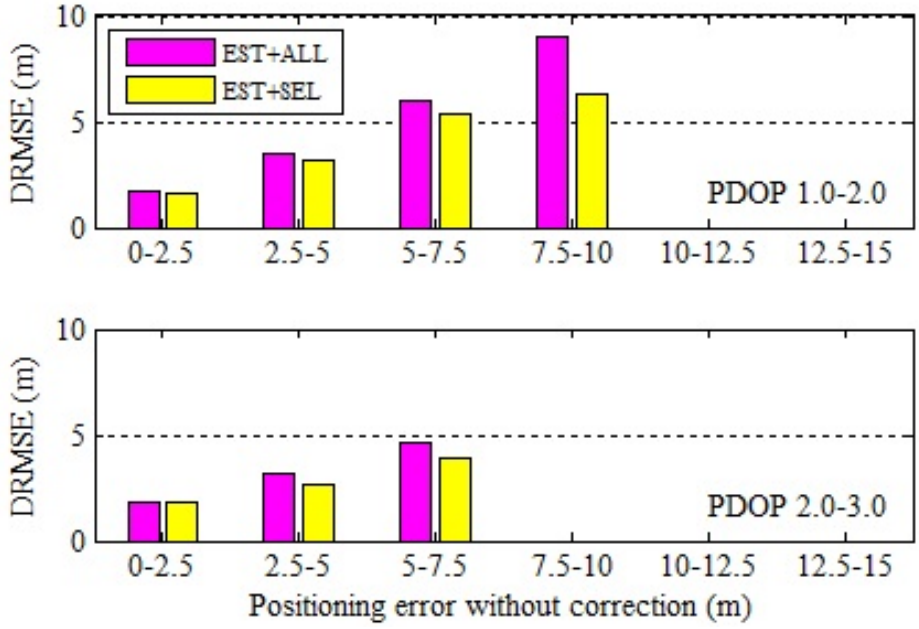

Figure 6.5 Effect of satellite selection for GPS+GLONASS positioning with ionosphere delay estimation for stormy period at station A

DRMSE by 65%. At station D, proposed selection algorithm reduces the DRMSE by 60%. At station E, proposed selection algorithm reduces the DRMSE by 19%. Thus, the satellite selection can improve the quality of positioning by removing the measurements of satellites which seems to be highly affected by ionospheric activity.

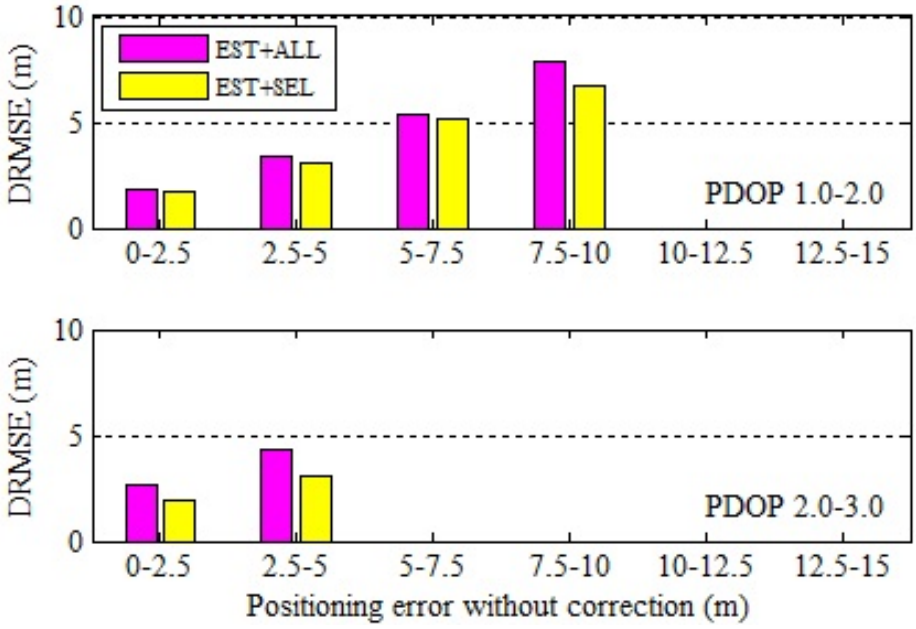

Figure 6.6 Effect of satellite selection for GPS+GLONASS positioning with ionosphere delay estimation for stormy period at station B

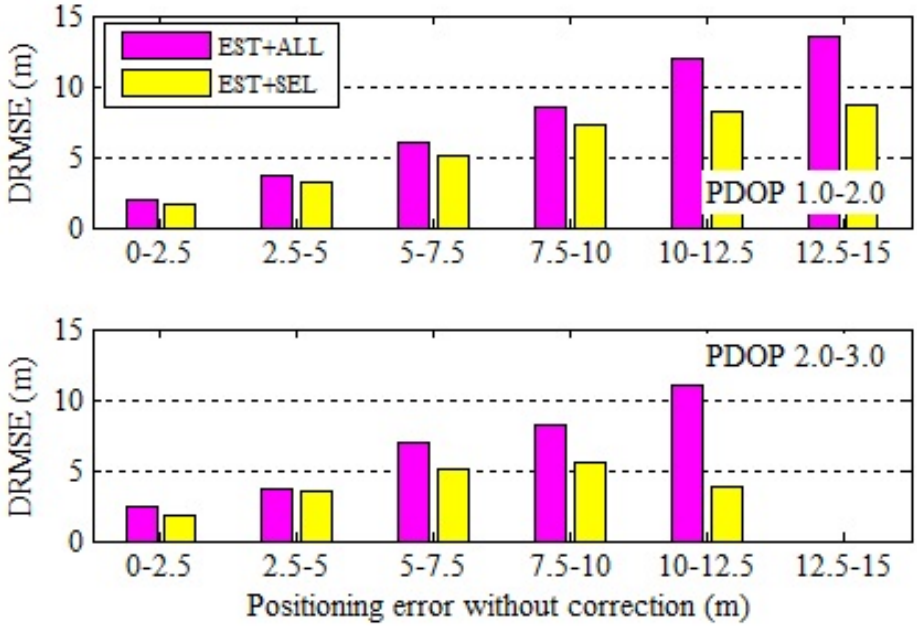

Figure 6.7 Effect of satellite selection for GPS+GLONASS positioning with ionosphere delay estimation for stormy period at station C

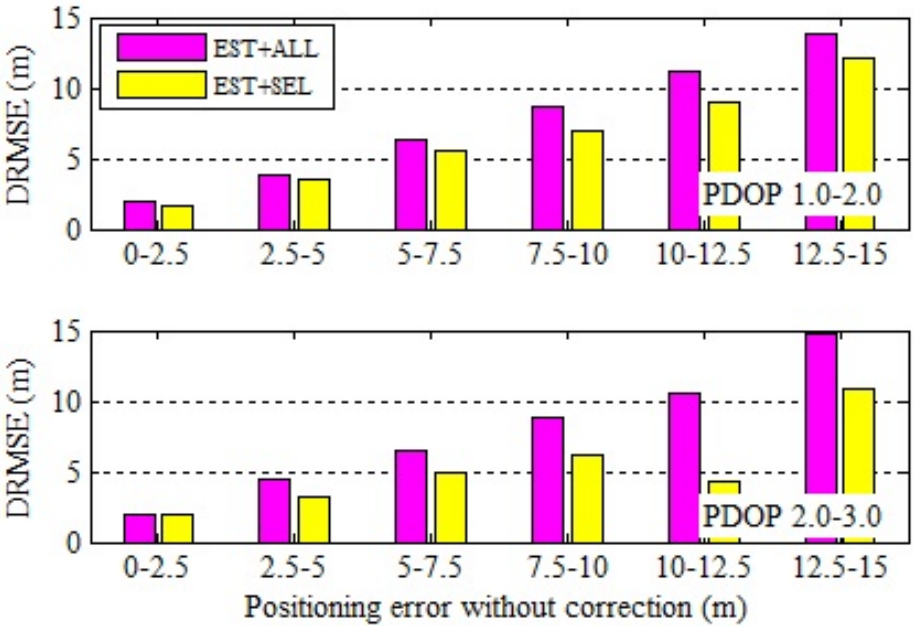

Figure 6.8 Effect of satellite selection for GPS+GLONASS positioning with ionosphere delay estimation for stormy period at station D

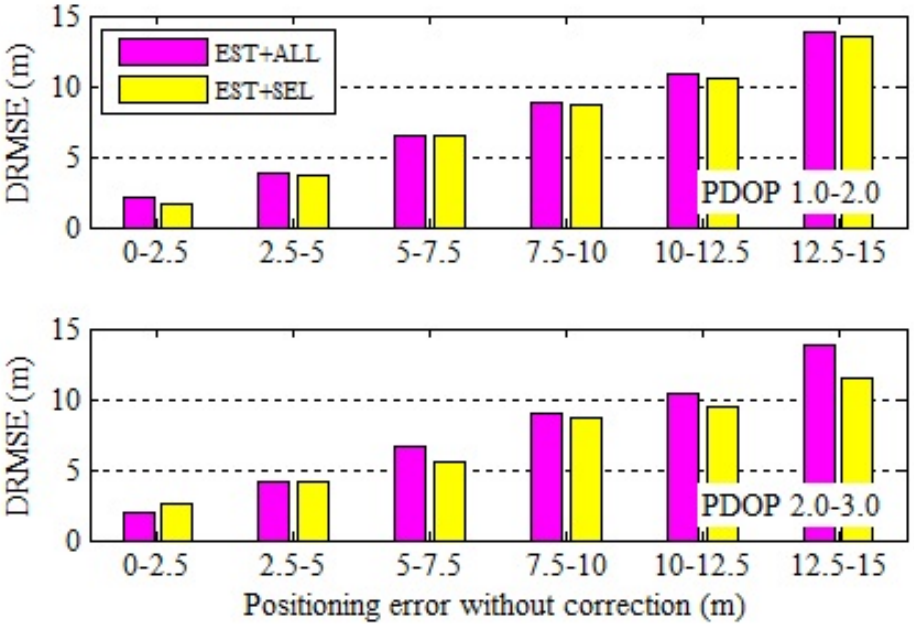

Figure 6.9 Effect of satellite selection for GPS+GLONASS positioning with ionosphere delay estimation for stormy period at station E

6.2.2 Effect of Ionosphere Delay Estimation

Figure 6.10 shows the horizontal positioning error without ionospheric correction with all visible satellites (UNC+ALL) as the example. The measurements observed on 9 November, 2013 were used. "UNC+ALL" and "KLB+ALL" denotes the result of positioning without ionosphere delay correction and with conventional correction, respectively, using all visible satellites. "EST+SEL" denotes the result of positioning with proposed ionosphere delay estimation using selected satellites. The positioning error is over 5 m during 12:00-21:00 in local time when the ionospheric delay seems to be large.

Figures 6.11 and 6.12 show the horizontal error reduction by conventional correction (KLB+ALL) and by proposed correction (EST+SEL), respectively, at station D on 9 November 2013. Although the ionospheric effect on positioning is large in daytime, the effectiveness of conventional method is not indicated. The result of the proposed method indicates its effectiveness in daytime.

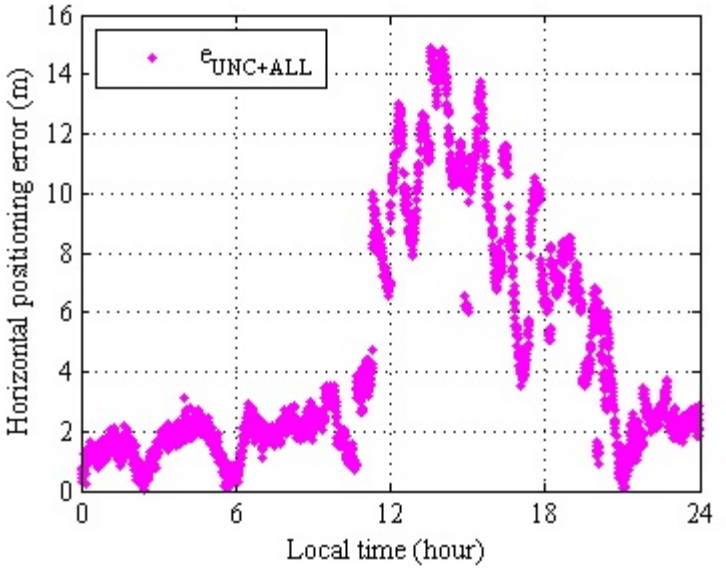

Figure 6.10 Horizontal positioning error of UNC+ALL at station D on 9 November, 2013

Figures 6.13 through 6.17 compare the DRMSE for GPS+GLONASS positioning with ionosphere delay correction for stormy period at selected five stations in Japan. When the ionospheric effect on positioning is small ($e_{uncorr} < 5$ m), the correction effects of both conventional and proposed methods on error reduc-

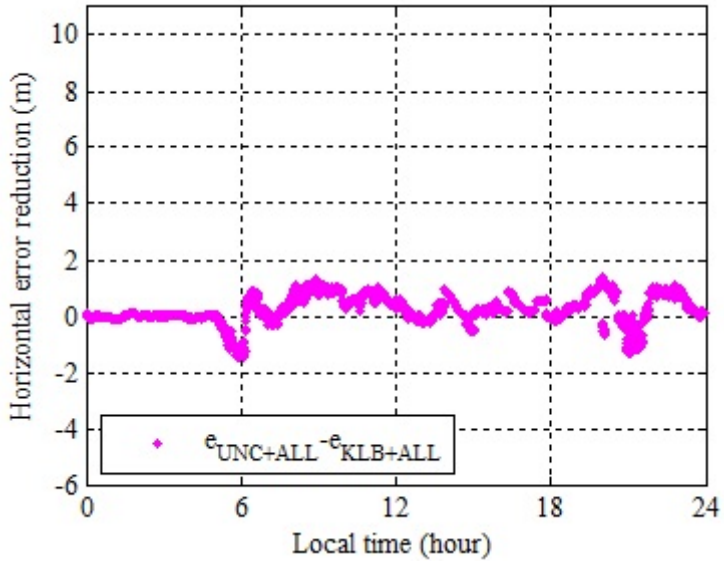

Figure 6.11 Horizontal error reduction by conventional correction (KLB+ALL) at station D on 9 November, 2013

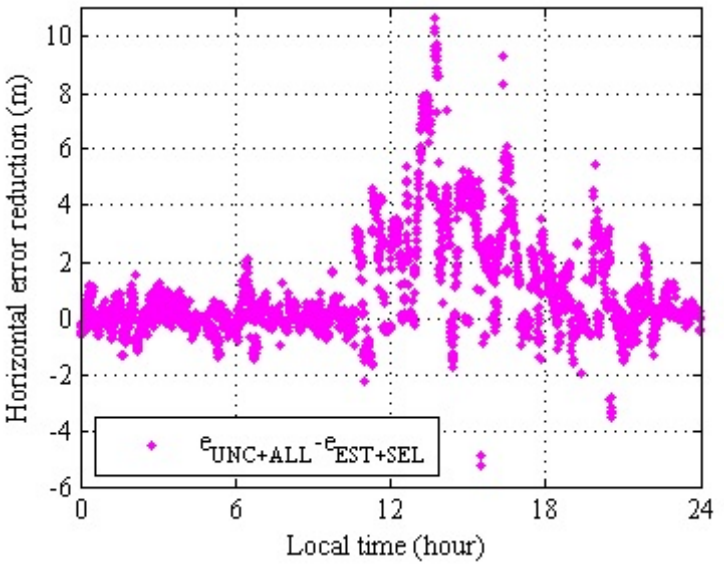

Figure 6.12 Horizontal error reduction by proposed correction (EST+SEL) at station D on 9 November, 2013

tion are reasonably small. In some cases, it is observed that the DRMSE value of e_{uncorr} is smaller than that of e_{corr}. It is not observed that the effectiveness of proposal is degraded in the case of PDOP 2.0-3.0, compared with that in the case of PDOP 1.0-2.0. Thus, the effectiveness of satellite selection is enlarged in the case of bad satellite constellation.

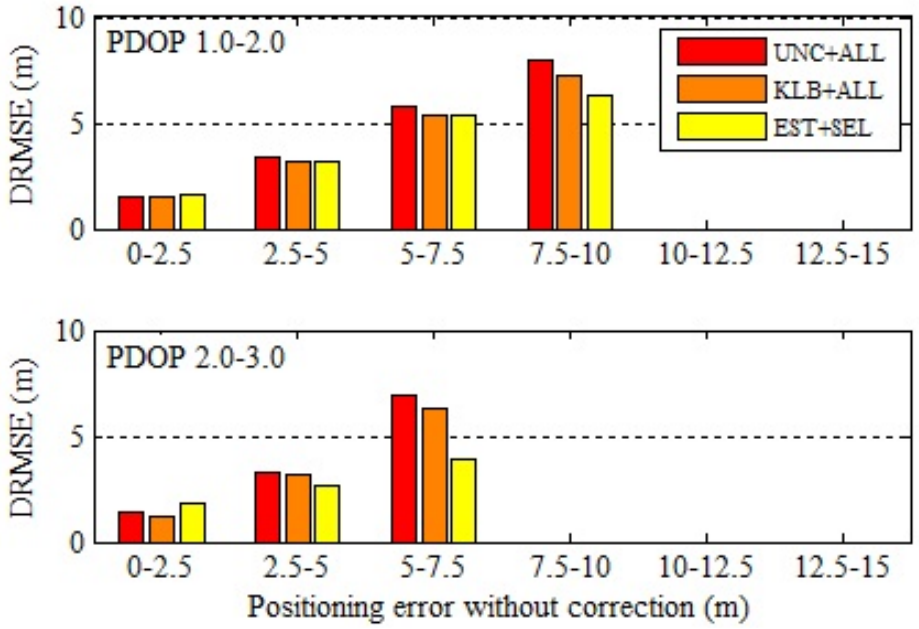

Figure 6.13 Comparison of DRMSE for GPS+GLONASS positioning with ionosphere delay correction for stormy period at station A

As it was discussed in section 3.1.2, ionospheric effect is relatively small at high latitude region. The result of station A and B show that the proposed correction method is effective and reduces the DRMSE when e_{uncorr} is over 5 m. The result of station C and D also show that the proposed method is highly effective when e_{uncorr} is over 7.5 m.

At station A, proposed selection algorithm reduces the DRMSE by 38%. At station B, proposed selection algorithm reduces the DRMSE by 6%. At station C, proposed selection algorithm reduces the DRMSE by 61%. At station D, proposed selection algorithm reduces the DRMSE by 57%. At station E, proposed selection algorithm reduces the DRMSE by 14%.

From the result of station E, we found that the correction effect of proposed method is not expected. The following reason can be considered. The ionosphere is more disturbed at region nearer from equation. At low latitude region,

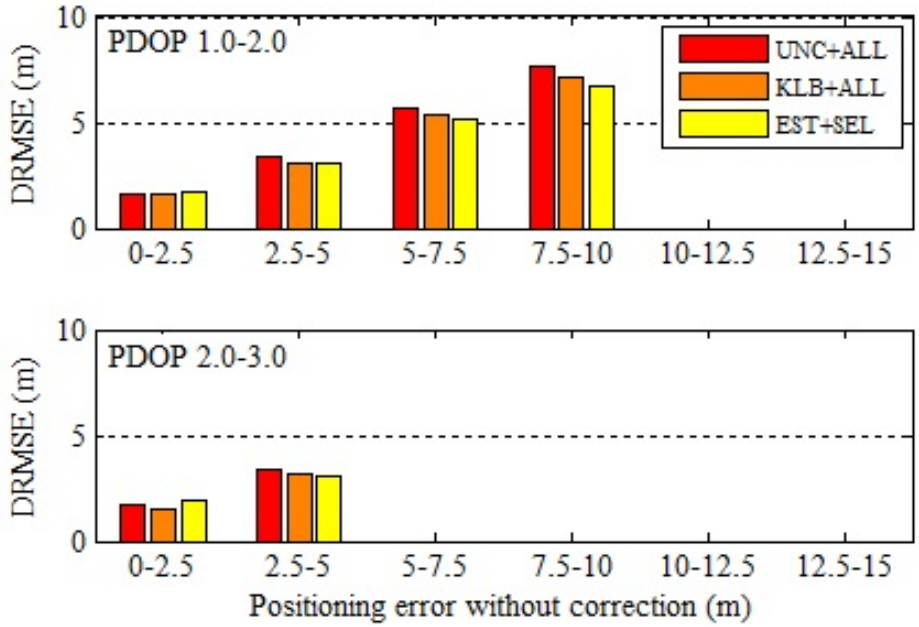

Figure 6.14 Comparison of DRMSE for GPS+GLONASS positioning with ionosphere delay correction for stormy period at station B

the GNSS signal, which propagates near from equation, can be observed. However, the ionospheric thin shell model introduced in this work assumes that the electron density is uniformly distributed. Thus, the possible solution is introducing the ionospheric model considering the distribution of electron density.

6.2.3 Drawback

There are times when the error reduction by proposed estimation method is almost zero or negative in daytime, as shown in Fig. 6.12. That is a drawback of the ionosphere delay estimation using single-frequency pseudorange measurements. The possible reasons for small error reduction is that the contribution of modeling error or measurement noise to measurement is large. Proposed selection algorithm try to remove the satellite measurement including those error. However, if the residual errors are large overall, it is sometimes unavoidable that the estimation error of ionosphere delay is large.

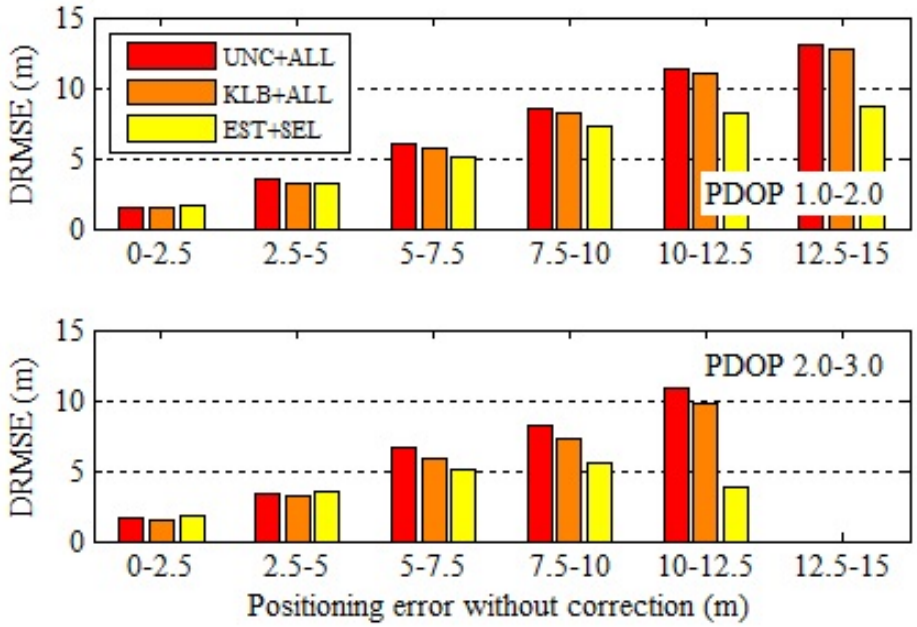

Figure 6.15 Comparison of DRMSE for GPS+GLONASS positioning with ionosphere delay correction for stormy period at station C

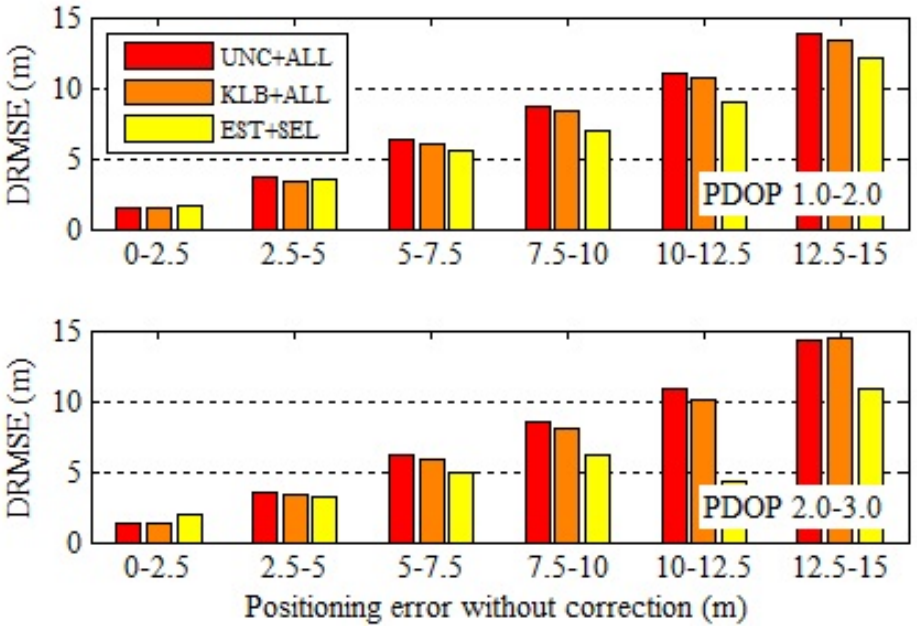

Figure 6.16 Comparison of DRMSE for GPS+GLONASS positioning with ionosphere delay correction for stormy period at station D

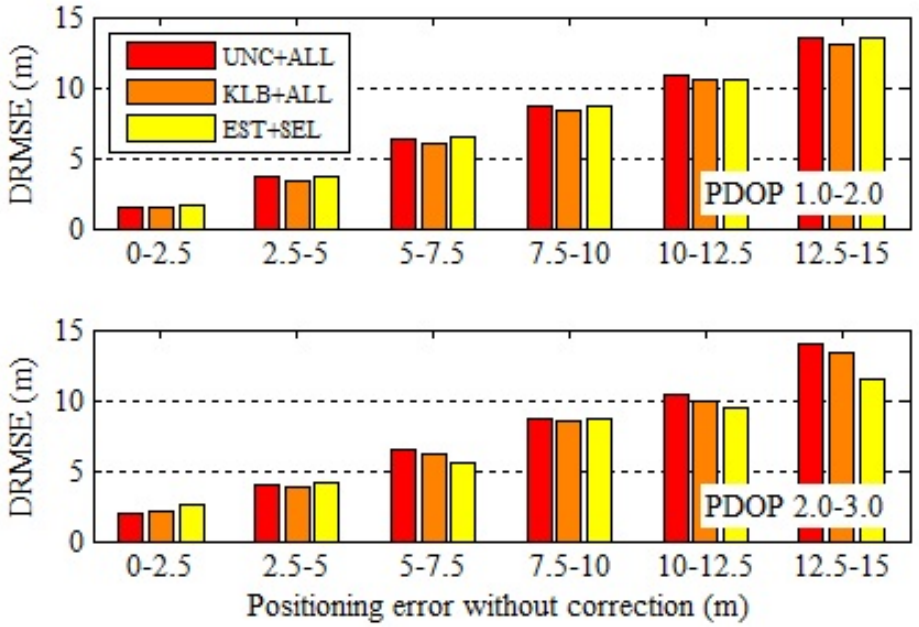

Figure 6.17 Comparison of DRMSE for GPS+GLONASS positioning with ionosphere delay correction for stormy period at station E

6.3 Comparative Evaluation of Positioning with Each Method

This section summarizes the performances of single- and multi-GNSS positioning with ionosphere delay correction methods with satellite selection. Table 6.2 summarizes the probability of best method of which the positioning error is minimum for stormy period when $e_{SGL+UNC+ALL}$ >5 m. The name of correction method in Table 6.2 is separated in three parts. The first term is "SGL" or "MLT", indicating positioning using single-GNSS (only GPS) or one using multi-GNSS (GPS+GLONASS), respectively. The second term denotes the correction method, "UNC", "KLB", or "EST". The third term are "ALL" or "SEL", indicating the positioning with all visible satellites or one with selected satellites.

At station A, B, and E, it is multi-GNSS positioning with conventional correction (MLT+KLB) that reduces the positioning error most with highest probability, while it is multi-GNSS positioning with proposed ionosphere delay estimation with satellite selection (MLT+EST+SEL) at station C and D.

Figures 6.18 through 6.22 compare the DRMSE for GPS and GPS+GLONASS positioning with various ionosphere delay correction for stormy period at selected five stations in Japan. This statistics is based on the value of PDOP for GPS positioning. When the largest bias error b_{ion} is small (e_{uncorr} <5 m), There is small advantage in using GLONASS of which b_{orb} and b_{sclk} are large (see Table 2.2). At station A, conventional method (MLT+KLB+ALL) keeps stable performance of ionospheric correction. When e_{uncorr} is within a range of 12.5< e_{uncorr} <15 m), the proposal (MLT+EST+SEL) has an ability to cor-

Table 6.2 The probability of best method of which the positioning error is minimum ($e_{SGL+UNC+ALL} > 5$ m)

Correction method	Station A	B	C	D	E
SGL+UNC+ALL	6%	2%	10%	14%	5%
SGL+KLB+ALL	8%	8%	7%	9%	16%
SGL+EST+ALL	27%	30%	17%	20%	19%
MLT+UNC+ALL	4%	5%	1%	3%	5%
MLT+KLB+ALL	38%	36%	19%	12%	24%
MLT+EST+ALL	0.3%	5%	2%	5%	11%
MLT+EST+SEL	15%	16%	43%	38%	21%

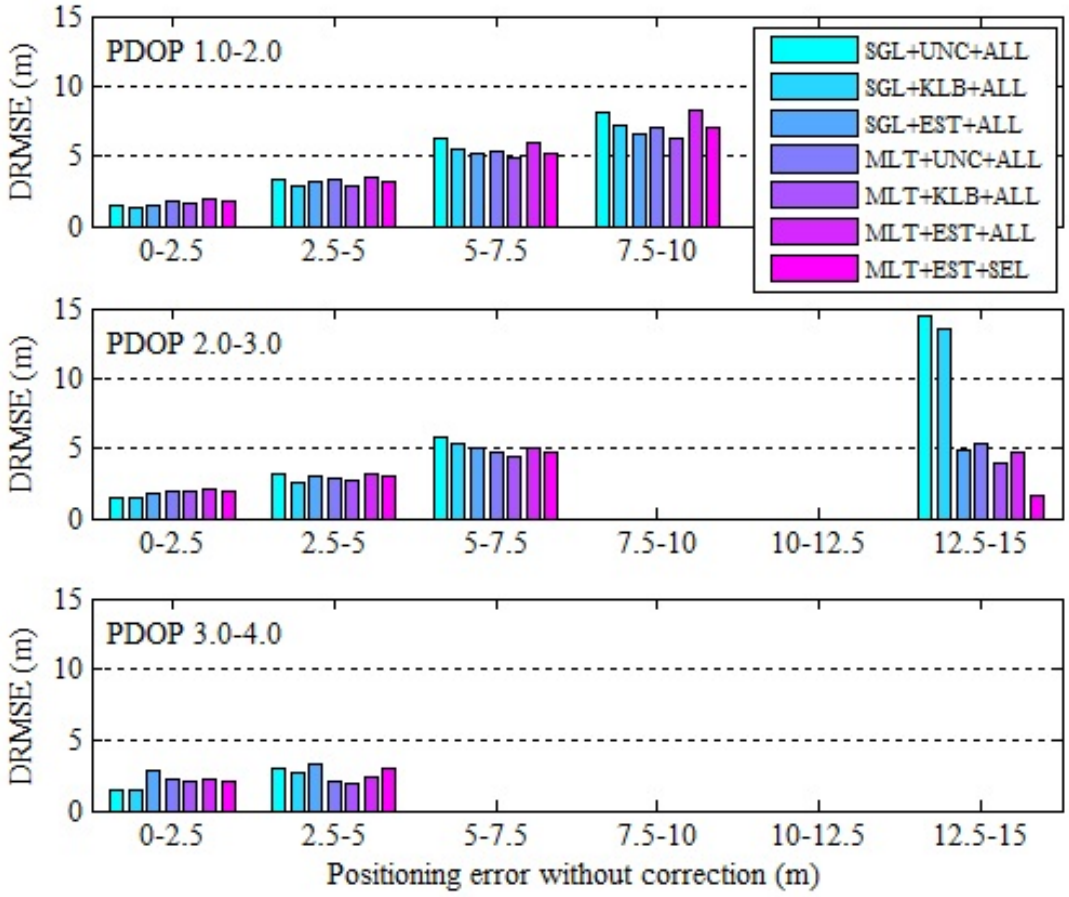

Figure 6.18 Comparison of DRMSE for GPS and GPS+GLONASS positioning with various ionosphere delay correction for stormy period at station A

rect large error. The result of station B shows in Fig. 6.19 and table 6.2 that MLT+KLB+ALL and SGL+EST+ALL have an equal ability. At station C, the probability of best method of MLT+EST+SEL is remarkably high. Moreover, it is highly effective especially when e_{uncorr} >10 m. The result of station D in Fig. 6.21 shows that proposed SGL+EST has an ability to correct large error (e_{uncorr} >7.5 m). Single-GNSS positioning has smaller value of DRMSE when e_{uncorr} <5 m at station E.

From these results, the reliable single-GNSS receiver requires to select the best method from all selectable positioning algorithm. The possible index of selection is the estimation value of ionosphere delay and its standard deviation.

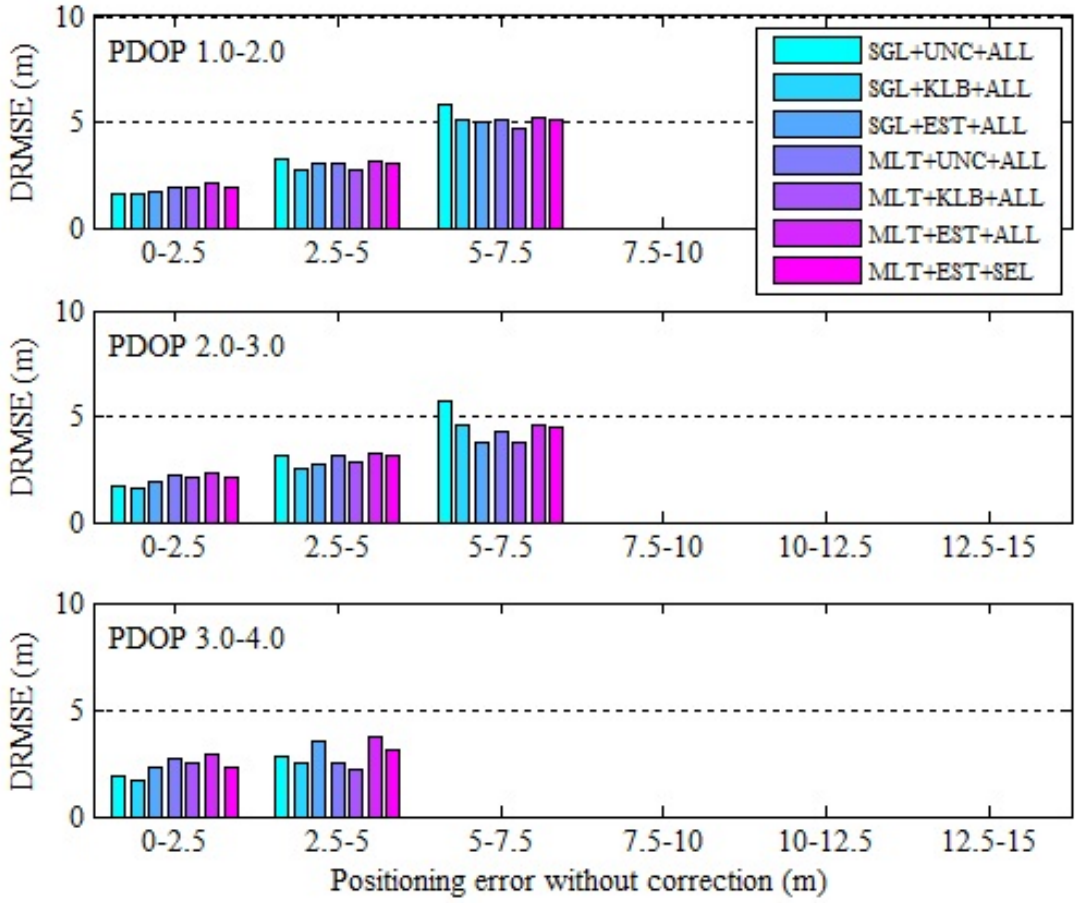

Figure 6.19 Comparison of DRMSE for single- and multi- GNSS positioning for stormy period at station B

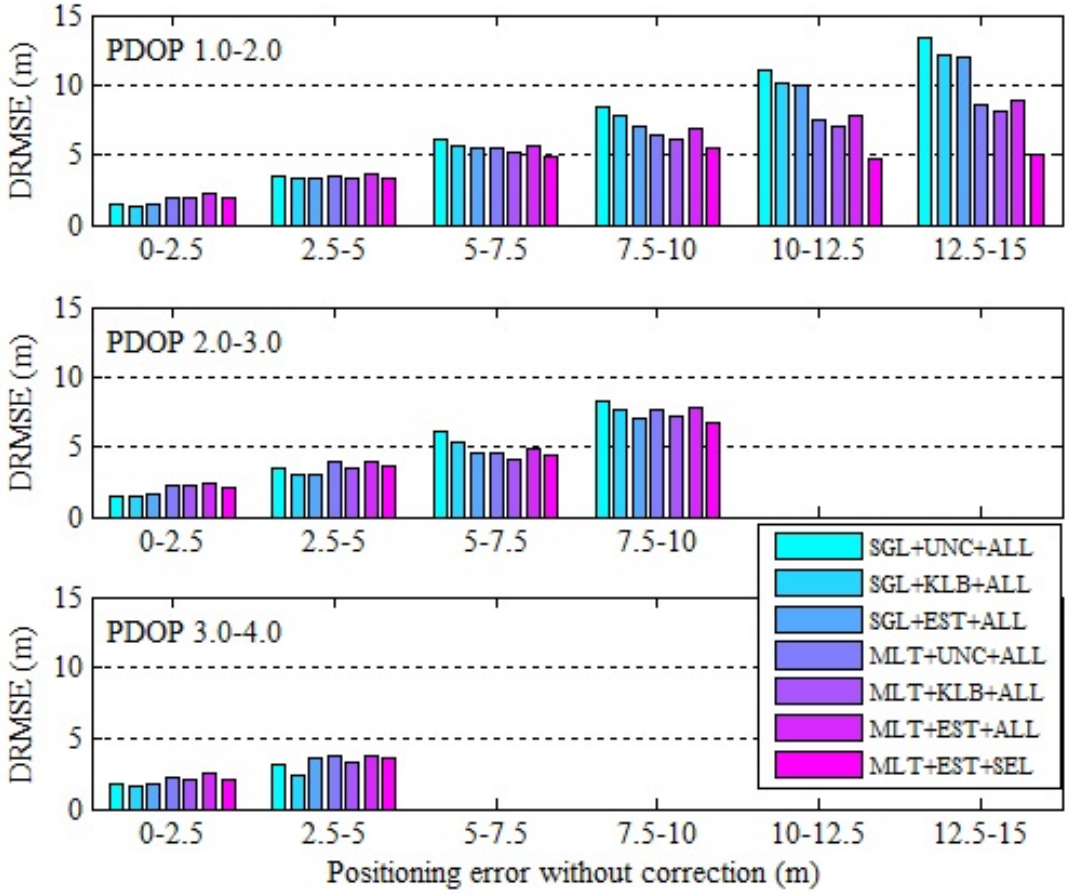

Figure 6.20 Comparison of DRMSE for single- and multi- GNSS positioning for stormy period at station C

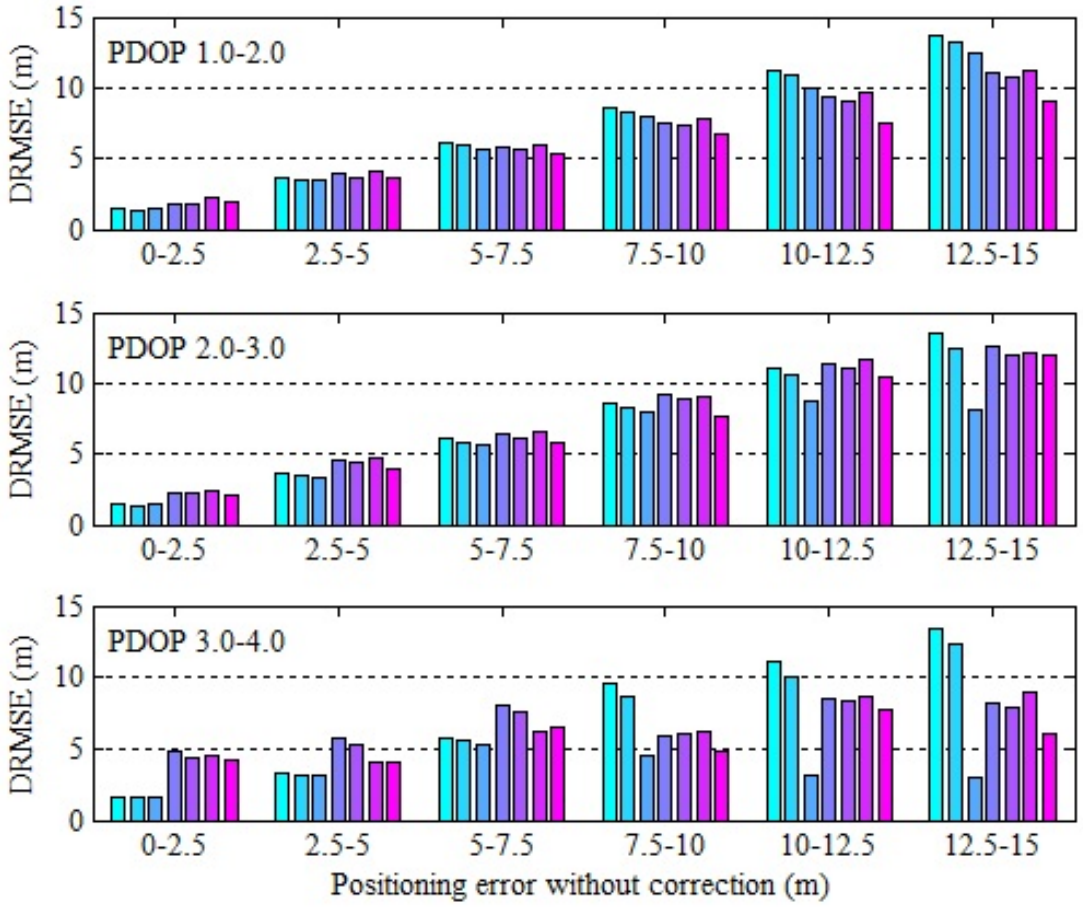

Figure 6.21 Comparison of DRMSE for single- and multi- GNSS positioning for stormy period at station D

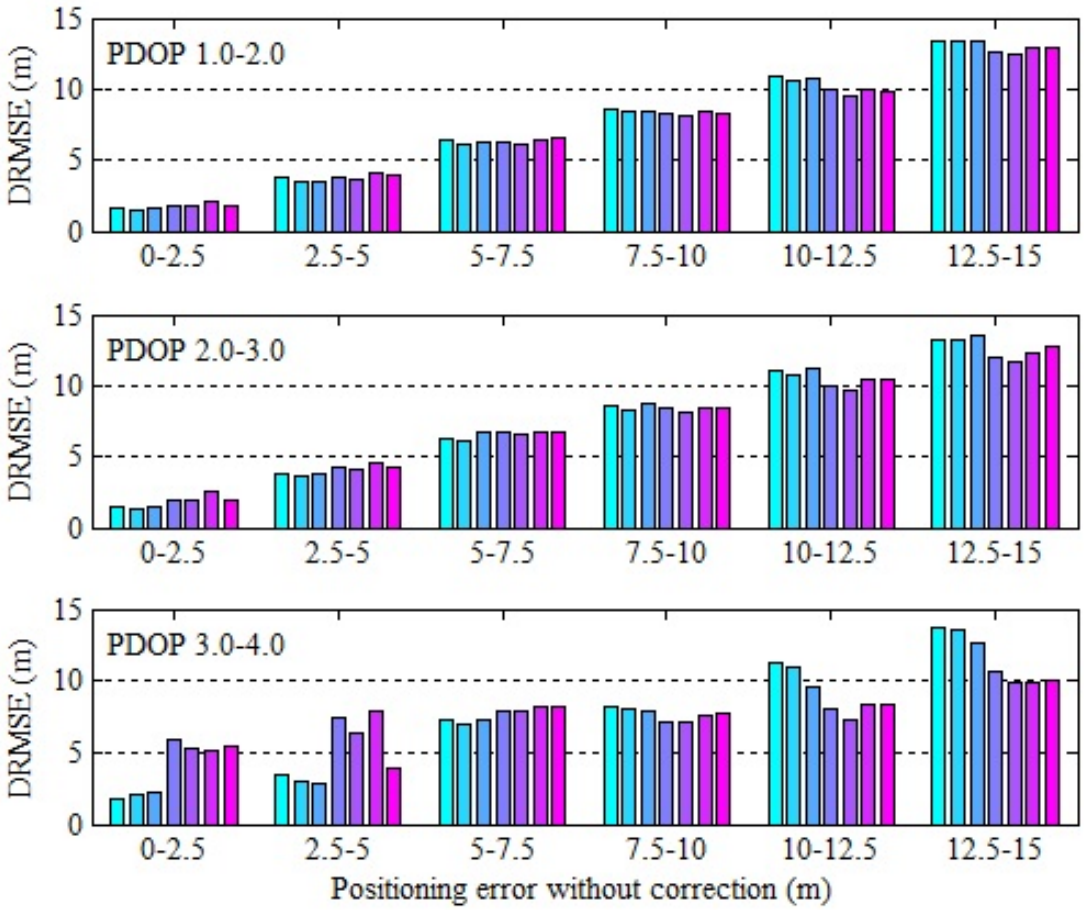

Figure 6.22 Comparison of DRMSE for single- and multi- GNSS positioning for stormy period at station E

Chapter 7

Conclusion

7.1 Summary

We proposed new method to mitigate the ionospheric effect on single-frequency GNSS positioning. Chapter 4 described the algorithm for estimating the ionosphere delay in real time. By representing the slant ionosphere delay by vertical delay and mapping function depending on the satellite elevation angle, the vertical delay can be estimated with receiver position and receiver clock offset. The numerical evaluation of its performance was conducted by using measurements of GPS observed at five stations in Japan for both ionospheric quiet and disturbed condition during a period from 2013 to 2015. The appropriate parameter of the height of ionospheric thin-shell for the ionospheric thin-shell model was studied. The result showed that setting the lower height was the best for the estimation using only pseudorange measurements of single epoch.

Chapter 5 discussed the effect of proposed ionosphere delay estimation method on positioning error reduction for GPS positioning by numerical evaluation. The results showed that it is effective when the ionospheric effect is large; in daytime and in lower latitude region. However, the correction effect at southernmost station was lower than expected. In order to avoid the adverse effect and to enhance the positive effect on error reduction, the suitable model for low-latitude region should be studied.

We also applied proposed ionosphere delay estimation to the multi-GNSS positioning combining GPS and Russian GLONASS. In order to estimate the delay more precisely, we proposed satellite selection algorithm, selecting satellite measurement which is suitable for positioning, in Chapter 6. The absolute value of residual ranging error between measurement and estimated value of pseudorange was used as the evaluation index for selecting satellites. The effective-

ness of satellite selection and ionosphere delay estimation for GPS+GLONASS positioning was indicated by numerical evaluation. Our proposed selection algorithm reduced the rms of horizontal error at almost all stations for stormy period in daytime. We also conducted the comparative evaluation of conventional and proposed ionosphere delay correction for GPS and GPS+GLONASS positioning. For high reliability of single-frequency positioning, the receiver needs to select the best method from all selectable positioning algorithm.

7.2 Future Work

For practical evaluation for performance of our proposed method, we need to apply it to the smartphone, drone, and some other mobile devices. Google released Android N in 2016 which outputs the raw GPS measurements. Then, we will easily demonstrate the effectiveness of our proposed algorithm for smartphone. We used the data observed at station where there is nothing to shield antenna from the satellite signals. If the proposed selection algorithm applies to the data observed in which there are buildings in one direction to shield it, it is expected that it is more effective than simply setting high elevation mask. Then, the effect of satellite selection in a multipath environment should be studied.

Published Papers

Reviewed Journal Papers

(1) Natsuki Kinugasa, Fujinobu Takahashi, Ryuji Kohno, "Mitigation of Ionospheric Effect on Multi-GNSS Positioning with Ionosphere Delay Estimation Using Single-Frequency Measurements of Selected Satellites," Journal of Aeronautics, Astronautics and Aviation (JoAAA), vol. 49, no. 2, Jun. 2017.

(2) Natsuki Kinugasa, Fujinobu Takahashi, Ryuji Kohno, "Improvement in Ionospheric Correction for Single-Frequency GNSS Positioning," International Journal of Trend in Research and Development (IJTRD), vol. 3, iss. 6, pp. 516-520, Dec. 2016.

Reviewed International Conference Papers

(1) Natsuki Kinugasa, Fujinobu Takahashi, Ryuji Kohno, "Estimation of Ionosphere Delay in Real Time by Single-Frequency Receiver for Single Point Positioning," Proceedings of International Symposium on GNSS 2015 (ISGNSS 2015), pp. 599-605, 2015.

International Conference Papers

(1) Natsuki Kinugasa, Fujinobu Takahashi, Ryuji Kohno, "Mitigation of Ionospheric Effect on Multi-GNSS Positioning with Ionosphere Delay Estimation Using Single-Frequency Measurements of Selected Satellites," International Symposium on GNSS 2016 (ISGNSS2016), Tainan, Taiwan, Dec. 6, 2016.

(2) Natsuki Kinugasa, Ryuji Kohno, "Ionospheric Effect on Measurement of QZSS and BeiDou," International Symposium on GNSS (ISGNSS 2014), Jeju, Korea, pp. 556-559, 24 Oct. 2014.

(3) Natsuki Kinugasa, Fujinobu Takahashi, "Ionospheric Electron Density Distribution Model for TEC Observation by QZSS and BeiDou," Asia Oceania Geosciences Society 11th Annual Meeting (AOGS 2014), Sapporo, Japan, Jul. 29, 2014.

(4) Natsuki Kinugasa, Takuto Shimizu, Tatsuhiro Muto, Toru Kajiwara, Fujinobu Takahashi, "Quasi-Zenith Satellite Observations for Total Electron Content of Plasmasphere and Ionosphere," American Geophysical Union Fall Meeting (AGU 2012), San Francisco, USA, Dec. 3, 2012

Domestic Conference Papers

(1) Natsuki Kinugasa, Fujinobu Takahashi, Ryuji Kohno, "Estimation for Total Electron Content Using Multi-GNSS," MTI Research Group Annual Meeting 2016, Tokyo, August 29, 2016. (in Japanese)

(2) Natsuki Kinugasa, Fujinobu Takahashi, Ryuji Kohno, "Estimation of Ionosphere Delay in Real-Time for Single Point Positioning by Single-Frequency Receiver," The Institute of Positioning, Navigation and Timing of Japan Annual Conference (IPNTJ2015), Tokyo, Apr. 24, 2015. (in Japanese)

(3) Natsuki Kinugasa, Fujinobu Takahashi, "Total Electron Content Observation by Using GPS, QZSS and BeiDou," Japan Geoscience Union Meeting (JpGU2014), PEM36-P24, Chiba, Apr. 28, 2014. (in Japanese)

(4) Natsuki Kinugasa, Fujinobu Takahashi, "Study of Ionospheric Electron Density Distribution Model for Multi-GNSS TEC Observation," The Institute of Positioning, Navigation and Timing of Japan Annual Conference (IPNTJ2014), Tokyo, Apr. 25, 2014. (in Japanese)

(5) Natsuki Kinugasa, Fujinobu Takahashi, "Method of Measuring Total Electron Content of Ionosphere by QZSS and BeiDou," Symposium on GPS/GNSS 2013, Tokyo, Oct. 31, 2013. (in Japanese)

(6) Natsuki Kinugasa, Fujinobu Takahashi, "Observation of Total Electron Content of Plasmasphere and Ionosphere by Using Multi-GNSS," 57th 第57回宇宙科学技術連合講演会 (JSASS2013), JSASS-2013-4617, Yonago, Oct. 11, 2013. (in Japanese)

(7) Natsuki Kinugasa, Fujinobu Takahashi, "Total Electron Content of Plasmasphere and Ionosphere Before and After Geomagnetic Storm by Using Quasi-Zenith Satellite," Japan Geoscience Union Meeting (JpGU2013), PEM29-P06, Chiba, May 22, 2013. (in Japanese)

(8) Natsuki Kinugasa, Fujinobu Takahashi, "Total Electron Content of Plasmasphere and Ionosphere Measured by Quasi-Zenith Satellite," Symposium on GPS/GNSS 2012, Tokyo, Oct. 26, 2012. (in Japanese)

(9) Natsuki Kinugasa, Takuto Shimizu, Tatsuhiro Muto, and Fujinobu Takahashi, "TEC Measurements Using Propagation Delay Difference of Two-Frequency Signal of QZS," Japan Geoscience Union Meeting (JpGU2012), Chiba, May 23, 2012. (in Japanese)

(10) Natsuki Kinugasa, Fujinobu Takahashi, "準天頂衛星 2 周波電波遅延差を利用した電離層全電子数計測," Symposium on IVS TDC (IVS2012), Kashima, Feb. 23, 2012. (in Japanese)

IEICE Annual Conference Letters

(1) Natsuki Kinugasa, Fujinobu Takahashi, "Total Electron Content of Ionosphere and Plasmasphere Measured by Quasi-Zenith Satellite," IEICE Society Conference 2012, no.B-2-29, Toyama, Sep. 13, 2012. (in Japanese)

(2) Natsuki Kinugasa, Takuto Shimizu, Tatsuhiro Muto, Fujinobu Takahashi, "TEC Measurements Using Propagation Delay Difference of Two-Frequency Signal of QZS," IEICE General Conference 2012, Okayama, Mar. 20, 2012. (in Japanese)

Bibliography

[1] D.J. Allain, C.N. Mitchell, "Ionospheric delay corrections for single-frequency GPS receivers over Europe using tomographic mapping," GPS Solut., vol. 13, iss. 2, pp. 141-151 (2009).

[2] C.O. Andrei, R. Chen, H. Kuusniemi, M. Hernandez-Pajares, J.M. Juan, D. Salazar, "Ionosphere effect mitigation for single-frequency precise point positioning," Proc. Int. Mtg. of the Satellite Division of The Institute of Navigation, Savannah, pp. 2508-2517 (2009).

[3] A. Cameron, "Google opnes up GNSS pseudoranges," GPS World, June 2016. http://gpsworld.com/google-opens-up-gnss-pseudoranges/, (cited 6 October 2016)

[4] W.A. Feess, S.G. Stephems, "Evaluation of GPS ionospheric time-delay model," IEEE Trans. Aerospace Electron Syst, vol. AES-23, iss. 3, pp. 332-338 (1987).

[5] J.A. Klobuchar, "Ionospheric time-delay corrections for advanced satellite ranging systems," Proc. NATO AGARD Conf., no. 209 (1976).

[6] N. Kinugasa, F. Takahashi, R. Kohno, "Estimation of ionosphere delay in real time by single-frequency receiver for single point positioning," Proc. Int. Symposium on GNSS 2015, Kyoto, pp. 599-605 (2015).

[7] N. Kinugasa, F. Takahashi, R. Kohno, "Improvement in ionospheric correction for single-frequency GNSS positioning," International Journal of Trend in Research and Development (IJTRD), vol. 3, iss. 6, pp. 516-520 (2016).

[8] N. Kinugasa, F. Takahashi, R. Kohno, "Mitigation of ionospheric effect on multi-GNSS positioning with ionosphere delay estimation using single-frequency measurements of selected satellites," Journal of Aeronautics, Astronautics and Aviation, *conditional acceptance*.

[9] Liu J, Chen R, Wang Z, Zhang H, "Spherical cap harmonic model for mapping and predicting regional TEC," GPS Solut., vol. 15, iss. 2, pp. 109-119 (2011).

[10] R.A. Scholtz, "Multiple access with time hopping impulse modulation," Proc. IEEE, Military Commun. Conf., pp.447-450, Boston, USA (1993).

[11] E.P. Macalalad, L.C. Tsai, J. Wu, C.H. Liu, "Application of the TaiWan ionospheric model to single-frequency ionospheric delay corrections for GPS positioning," GPS Solut vol. 17, iss. 3, pp. 337-346 (2013).

[12] P. Misra, P. Enge, "Global Positioning System: signals, measurements and performance second edition, " Massachusetts: Ganga-Jamuna press (2006).

[13] T. Ondo, K. Marubashi (ed), "Uchu Kankyo Kagaku (Science of space environment), " Tokyo: Ohmsha (2000).

[14] I.G. Petrovski, "GPS, GLONASS, Galileo, and BeiDou for mobile devices: from instant to precise positioning," Cambridge: Cambridge University press (2014).

[15] A. Yasuda, H. Yamada, "The role of QZSS in the era of multi-GNSS," IEICE Technical Report SANE 2011-31, pp. 83-88 (2011).

[16] T.P. Yunck, "Orbit determination. In: Parkinson BW (ed) Global positioning system: theory and applications," vol. 2, AIAA, pp.559-591 (1996).

[17] International GNSS Service (IGS), http://www.igs.org/products

[18] Navstar GPS Space Segment, "Global positioning systems directorate systems engineering & integration interface specification (IS-GPS-200)," (2013).

[19] Russian Institute of Space Device Engineering, "GLONASS interface control document, Navigational radiosignal In bands L1, L2 (edition 5.1)," Moscow (2008).

[20] Japan Aerospace Exploration Agency (JAXA), "Quasi-zenith satellite system user interfaces Ver. 1.6 (IS-QZSS)," (2014).

[21] International GNSS Service (IGS), "The receiver independent exchange format (Version 3.02)," (2013).